

**The Role of Amyloid Precursor Proteins: Studies using
Neurons generated from Wild-Type and Mutant
Embryonic Stem Cells**

Inauguraldissertation

zur
Erlangung der Würde eines Doktors der Philosophie
vorgelegt der
Philosophisch-Naturwissenschaftlichen Fakultät
der Universität Basel

von

Katrin Schrenk
aus Waldshut, Deutschland

Weilheim, Mai 2006

Genehmigt von der Philosophisch-Naturwissenschaftlichen Fakultät
auf Antrag von

Prof. Yves-Alain Barde

Prof. Markus Rüegg

Dr. Miriam Bibel

Basel, den 20.09.2005

Prof. Dr. Hans-Jakob Wirz

Dekan der Philosophisch
Naturwissenschaftlichen Fakultät

Ich erkläre, dass ich die Dissertation „The Role of Amyloid Precursor Proteins: Studies using Neurons generated from Wild-Type and Mutant Embryonic Stem Cells“ nur mit der darin angegebenen Hilfe verfasst und bei keiner anderen Universität und keiner anderen Fakultät der Universität Basel eingereicht habe.

Basel, 31.08.2005

Contents

Summary	2
1 Introduction	4
1.1 Alzheimer`s Disease (AD)	4
1.2 APP gene family	6
1.3 APP gene family members: possible synaptic functions	8
1.4 Aim of the thesis	9
2 Materials and Methods	10
2.1 Differentiation of embryonic stem (ES) cells	10
2.2 Immunostainings	15
2.3 Glutamate Release Assay	16
2.4 Western Blot	17
2.5 RT-PCR	18
2.6 Genotyping	22
3 Results	27
3.1 Isolation and characterization of embryonic stem cells lacking <i>app</i> and <i>aplp2</i>	27
3.2 Characterization of neural progenitors derived from ES cells lacking <i>app</i> or <i>app</i> and <i>aplp2</i>	34
3.3 Expression of synaptic proteins in neurons lacking <i>app</i> or <i>app</i> and <i>aplp2</i>	37
3.4 <i>VGLUT2</i> transcription in wild-type and <i>app</i> ^{-/-} <i>aplp2</i> ^{-/-} neurons	41
3.5 Release of glutamate in wild-type and <i>app</i> ^{-/-} <i>aplp2</i> ^{-/-} neurons	44
3.6 <i>VGLUT2</i> transcription after γ -secretase inhibitor treatment	48
3.7 Levels of <i>VGLUT2</i> protein and RNA in neurons expressing human APP in addition to endogenous mouse APP	50
4 Discussion	54
4.1 Vesicular glutamate transporters (VGLUTs)	54
4.2 Changes of PSD-95 in neurons lacking <i>app</i> and <i>aplp2</i>	58
4.3 The APP intracellular domain and transcriptional modulation	59
4.4 Synaptic changes in mice lacking <i>app</i> and <i>aplp2</i>	62
5 References	64
6 Acknowledgements	70
7 Curriculum Vitae	71

Summary

Alzheimer's Disease (AD) is the most common neurodegenerative disorder in elderly people. It is becoming an ever larger problem due to prolonged life-expectancies in developed countries. One of the central pathological hallmarks of the disease are deposits of aggregated amyloid β ($A\beta$), a peptide proteolytically derived from the amyloid precursor protein (APP). Although the contribution of APP to the pathology of AD has been at the center of most AD research for about two decades, the physiological role of this membrane protein still remains elusive. *APP* belongs to a conserved gene family including the amyloid precursor-like proteins 1 and 2 (APLP1 and APLP2). While mice lacking individual genes do not display any overt phenotype, double *null* mutations for *app* and *aplp2* result in early postnatal lethality, at the time when neuronal activity begins to be essential. These findings suggest functional redundancy of APP and APLP2, which is further supported by their similar pattern of expression. In order to address the role of these genes during neuronal differentiation, we made use of a newly established method allowing the generation of uniform populations of neurons starting with cultured mouse embryonic stem (ES) cells. This protocol leads to the generation of an essentially pure population of neural progenitors defined as Pax6-positive radial glial cells. As known from recent cell lineage analyses *in vivo*, these progenitors give rise to essentially all pyramidal, glutamatergic neurons in the cerebral cortex and in the hippocampus. In this work, we made use of ES cells lacking both *app* and *aplp2* and compared some of the biochemical properties of neurons derived from such cells with those obtained from wild-type ES cells. In the absence of *app* and *aplp2*, we detected a marked reduction in the expression of one of the vesicular transporters for glutamate, VGLUT2. In line with this, we found that the reduction in transporter levels is functionally significant, as less glutamate was released from these neurons following depolarizing stimuli. With regard to possible mechanisms linking the transcription of *vglut2* and APP, we blocked γ -secretase activity in wild-type neurons and observed that inhibition of the generation of a soluble intracellular domain of APP (AICD) leads to a decrease in the transcription of *vglut2*.

The present work thus suggests a link between APP and the development of glutamatergic synapses. This may provide an explanation for the early postnatal lethality of animals lacking both *app* and *aplp2*.

Dysfunction of APP processing might also provide a mechanistic link explaining some of the synaptic alterations thought to occur in AD.

Introduction

1.1 Alzheimer's Disease (AD)

Alzheimer's disease is a neurodegenerative disorder leading to cognitive, memory and behavioral impairments. It is the most common form of dementia in people over 65 years of age and it will become an increasing health problem due to extended life-expectancies in developed countries. No cure or preventative therapy is available yet and the definitive diagnosis is still based on postmortem histopathological examinations of the brains of patients. Two types of aggregates characterize the disease: extracellular deposits of amyloid β ($A\beta$) peptide in senile plaques and intraneuronal neurofibrillary tangles formed by hyperphosphorylated tau (review de Strooper et al., 2000; review Tanzi et al., 2005).

While the vast majority of AD cases are sporadic, about 5% are caused by mutations (familial Alzheimer's Disease, FAD). Genetic studies on these inherited forms allowed considerable progress to be made with regard to possible mechanisms underlying the disease. Indeed, several mutations have been found in a gene encoding the amyloid precursor protein (APP). APP is a transmembrane protein known to be processed by two different cleavage pathways *in vivo* (Fig.1). In the predominant "non-amyloidogenic pathway", APP is cleaved by α -secretase within the $A\beta$ domain. A soluble extracellular fragment ($sAPP\alpha$) and a C-terminal fragment (C83) are produced. The latter can be further cleaved intramembranously by γ -secretase to produce a small peptide, P3 and the APP intracellular domain (AICD). In the "amyloidogenic pathway" APP is cleaved by β -secretase (BACE-1), leading to the generation of a soluble extracellular fragment ($sAPP\beta$) and of a C-terminal fragment (C99). C99 can be further processed by γ -secretase to release the AICD and $A\beta$. Both cleavage pathways take place under physiological conditions and therefore suggest that all fragments of APP, including $A\beta$, may be part of hitherto unrecognized, normal processes.

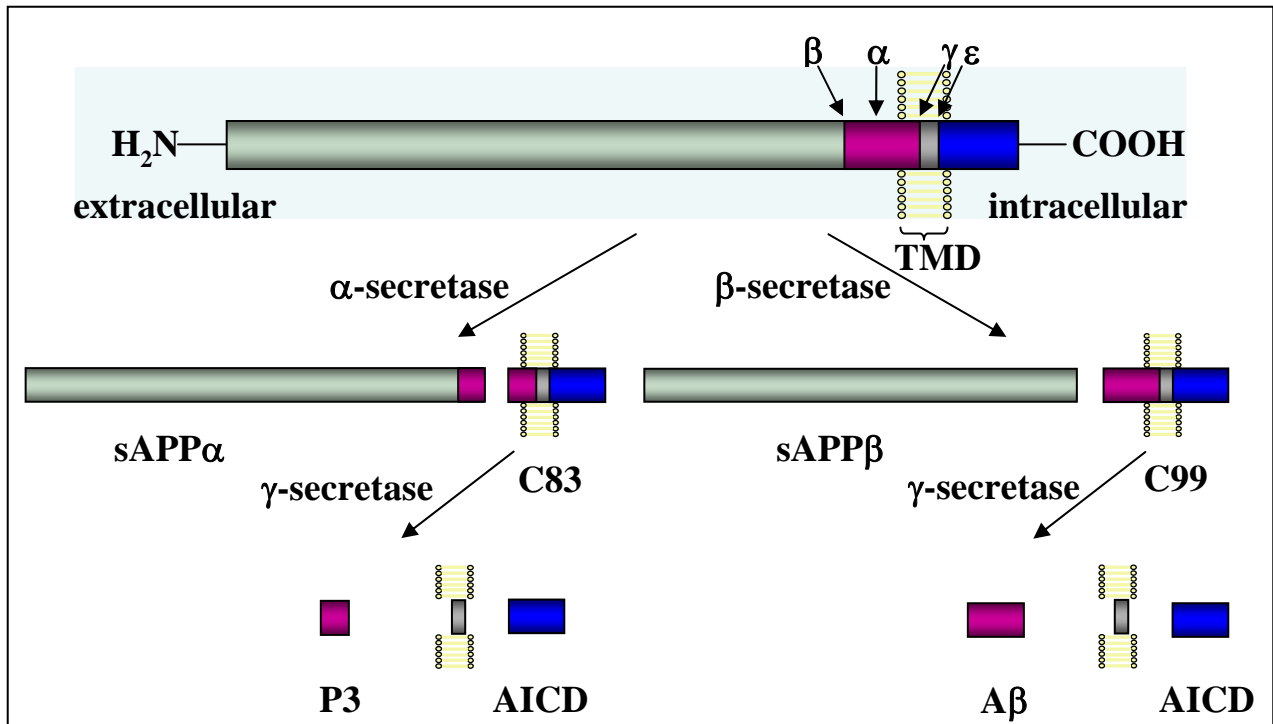


Figure 1: Cleavage schema of APP

APP is first cleaved by either α - or β -secretase releasing a soluble extracellular fragment (sAPP α or sAPP β). The remaining C-terminal fragments, C83 or C99, are further cleaved by γ -secretase resulting in the generation of either a small extracellular fragment P3 (after C83 cleavage) or A β (after C99 cleavage). In addition the APP intracellular domain (AICD) is released. (TMD = transmembrane domain)

The next breakthrough in the characterization of the mechanisms underlying AD came with the discovery of mutations in genes encoding for presenilin1 (PS1) and 2 (PS2), two related membrane proteins that have recently been identified as being part of the multiprotein proteolytic complex γ -secretase. The identification of PS1 and PS2 was a major finding with implications extending well beyond the field of AD. Indeed, both presenilins are also involved in the processing of other transmembrane proteins, including Notch in particular, the cleavage of which had remained a mystery before the identification of PS1 and PS2 (review Selkoe et al., 2002; review de Strooper, 2003).

An increase in the production of A β is common to most of the hereditary forms of AD. This is also illustrated by patients affected by Down syndrome (Trisomy 21). After the age of 40, the majority of them develop AD pathology with neuritic plaques and tangle formation. As the *APP* gene is localized on chromosome 21, Down syndrome patients harbor three copies of the *APP* gene and it seems that the increase in copy number may be sufficient to induce AD pathology.

Interestingly, mutations in the *tau* gene, encoding for the other protein found to be altered in the brain of AD patients, are not associated with Alzheimer's disease. Mutated tau can lead to frontotemporal dementia with parkinsonism (FTDP-17), another severe form of dementia which is characterized by widespread deposition of tangles but absence of amyloid plaques. Therefore FTDP-17 is not classified as AD (review de Strooper et al., 2000).

Taken together, the human genetics of AD points to APP and its processing being directly implicated in the pathology of the disease. While mutations in the corresponding genes only account for a relatively small percentage of AD cases, it is of interest that the pathological lesions in sporadic forms of AD are similar to those found in the hereditary forms. Therefore it can be assumed that changes in the processing of APP also play a role in the pathogenesis of the much more frequent, non-familial form. However, neither the physiological function of the fragments (related or not related to A β) generated by the proteolysis of APP, nor the physiological function of APP is known at this point. This latter question was the basis of the present work which we approached using a newly developed cell culture system allowing the generation of neurons from embryonic stem cells lacking APP and its relative APLP2.

1.2 APP gene family

The amyloid precursor protein belongs to a gene family that comprises 3 members in mammals: amyloid precursor protein (APP), amyloid precursor-like protein 1 (APLP1) and amyloid precursor-like protein 2 (APLP2). Homologues have also been found in the fruit fly *Drosophila melanogaster*, amyloid precursor protein like protein (APPL), and in the worm *Caenorhabditis elegans*, amyloid protein-like protein 1 (*apl-1*; review de Strooper et al., 2000).

All three proteins are type I transmembrane proteins with a large extracellular (~624-700 amino acids), a transmembrane (~25 amino acids) and a short intracellular (~46 amino acids) domain. They are clearly related in sequence, with a slightly closer similarity between APP and APLP2 (APLP1 versus APP: 42%; APLP2 versus APP: 52% and APLP1 versus APLP2: 43% amino acid identities in human; Wasco et al., 1992; Wasco et al., 1993). The main difference is the lack of the A β sequence in the two APP like proteins. Remarkably, no mutations associated with AD have been found in the *apl1* and *apl2* genes so far, a finding that further supports the view that A β is linked to AD, not least because

both, APLP1 and APLP2, are proteolytically processed in the same manner as APP (Lo et al., 1995; Paliga et al., 1997; Li et al., 2004).

With regard to the expression patterns of the three genes, APP and APLP2 mRNAs are found in largely overlapping patterns during embryogenesis and in adult tissue. They are expressed in the central and peripheral nervous system, as well as in most organs (Slunt et al., 1994). In the adult brain, the transcripts are found not only in the same brain regions, but also at similar levels. For example high levels are found in the temporal association cortex and lower levels in the hippocampus (Wasco et al., 1993). APLP1 is only found in the developing and adult central and peripheral nervous system, but not in non-neuronal tissue (Lorent et al., 1995).

The physiological function of APP and its homologues still remains unclear. A large body of *in vitro* experiments suggests a contribution of APP to multiple cellular processes including neurite outgrowth (Zheng et al., 1995; Sabo et al., 2003), neuronal survival (Perez et al., 1997), cell-cell adhesion (Yamazaki et al., 1997; Coulson et al., 2000), axonal transport (Kamal et al., 2000; 2001), cell proliferation (Ohsawa et al., 1999; Caille et al., 2004), synaptogenesis (Schubert et al., 1991; Moya et al., 1994; Morimoto et al., 1998; Kirazov et al., 2001; Kamenetz et al., 2003; Wang et al., 2005; Yang et al., 2005) and transcriptional regulation (Cao et al., 2001). Some of these functions have also been described for APLP1 and APLP2, such as neurite outgrowth (Thinakaran et al., 1995), synaptogenesis (Kim et al., 1995; Wang et al., 2005; Yang et al., 2005), cell proliferation (Caille et al., 2004) and transcriptional regulation (Scheinfeld et al., 2002).

To elucidate the physiological role of the *app* and *app*-related genes, mice deficient in either APP, APLP1 or APLP2 have been generated (Müller et al., 1994; Zheng et al., 1995; Li et al., 1996; von Koch et al., 1997; Heber et al., 2000). All single mutants are viable and fertile with only subtle neurological deficits in the case of APP deficiency, suggesting redundancy of function among the APP gene family members. This view is supported by the phenotypes of combined *null* mutants. The lack of APP and APLP2 or APLP1 and APLP2 results in early postnatal lethality (P0) without histopathological abnormalities in any of the organs examined including the brain. By contrast, the lack of APP and APLP1 results in viable mice without any detectable phenotype (von Koch et al., 1997; Heber et al., 2000).

Why on the other hand the combination of *null* mutations in the *aplp1* and *aplp2* genes should be lethal if APP and APLP2 exert the same function remains unclear at this point and is not easy to explain.

1.3 APP gene family members: possible synaptic functions

The expression of APP and APLP2 is developmentally regulated and a strong increase in expression occurs at the time of synaptogenesis (Moya et al., 1994; Kirazov et al., 2001). These observations led to the hypothesis that both proteins may have a role in synapse formation and maturation. In addition, APP and APLP2 are transported to presynaptic sites by kinesin-I dependent fast anterograde axonal transport (Koo et al., 1990; Schubert et al., 1991). APP itself is thought to be involved in the transport mechanism by serving as a membrane cargo receptor for kinesin-I, linking this protein to a subset of other axonally transported vesicles, possibly including those containing molecules required for proper synaptic function such as neurotransmitter transporters (Kamal et al., 2000 and 2001).

Observations made with APP antibodies applied to primary hippocampal cultures further suggest a role of APP in synapse maturation and/or function (Morimoto et al., 1998). A decrease of spontaneous synchronous neuronal oscillations could be observed after antibody treatment of the neurons. These oscillations of $[Ca^{2+}]_i$ result from the spontaneous activity of neurons forming synapses, and the number of synchronized neurons was found to correlate with the number of synapses formed. Blocking APP with an antibody might therefore result in the inhibition of the formation of functional synapses.

Very recently, the notion that APP and APLP2 may be somehow involved in synaptic function received further support by two publications (Wang et al., 2005; Yang et al., 2005) indicating defects in synaptic structure and synaptic transmission in the neuromuscular junction and submandibular ganglia of mice lacking both genes (see Discussion).

1.4 Aim of the thesis

Given our lack of understanding of the role of APP and APLP2, as well as the early postnatal death of the double mutants, it would be desirable to investigate this question using cultured cells. Neuronal

cultures have been established from the embryonic brains of double knock-out animals, but they did not help to bring further insight into the role of APP and APLP2 (Heber et al., 2000). Both the inherent heterogeneity of such cultures, as well as the limited quantities of cells contribute to make biochemical assays and screens difficult.

In the present work, we took advantage of a novel cell culture protocol based on the use of mouse embryonic stem (ES) cells (Bibel et al., 2004). Our laboratory has recently shown that homogeneous populations of glutamatergic neurons can be obtained from wild-type ES cells. As ES cells can be generated in unlimited quantities, they represent a potentially attractive model to study the consequences of selective gene deletion in differentiated neurons *in vitro*. ES cells were derived from blastocysts of *app/aplp2* double mutant animals and their differentiation into neurons was compared with that of wild-type ES cells using biochemical, molecular biological and functional methods.

Materials and Methods

2.1 Differentiation of embryonic stem (ES) cells

2.1.1 Feeder preparation

Feeder medium

	concentration	supplier
FCS	10%	Invitrogen, personal reservation, heat inactivated 30 min at 55°C
glutamine (200 mM)	0.8 mM	Invitrogen #25030-024
DMEM (+ high glucose + sodium pyruvate - glutamine)	to final volume	Invitrogen #21969-035

Embryos day 13.5-14.5 after gestation were decapitated and all inner organs, spinal cord and extremities were removed. The remaining tissue was cut into small pieces and incubated in 1 ml trypsin/0.5% EDTA (Invitrogen #25300-054) for 30 min at 37°C.

10 ml feeder medium were added for trypsin inactivation and after 5 min incubation the supernatant was transferred into a fresh tube. 10 ml feeder medium were added again to the remaining tissue-pellet and incubated for 5 min before the supernatant was collected. The procedure was repeated three times in total. The supernatant was filtered through a cell strainer (BD Falcon™ #352360; 100 µm pore size) and centrifuged for 5 min at 1000 rpm. The pellet was resuspended in feeder medium and plated on 150 cm² culture flasks (BD Falcon™ #355000), one embryo per two plates. The feeders were expanded once before aliquots were frozen.

2.1.2 Embryonic stem cell cultivation

ES medium

	concentration	supplier
FCS	15%	Invitrogen, personal reservation, heat inactivated 30 min at 55°C
non-essential amino acids (100x)	1x	Invitrogen #11140-035
Leukemia inhibitory factor (LIF)	10 ³ Units/ml	Chemicon, ESG1107, 10 ⁷ Units/ml
glutamine (200 mM)	0.8 mM	Invitrogen #25030-024
β-mercaptoethanol	0.001%	Sigma #M7522
DMEM	to final volume	Invitrogen #21969-035

Feeder cells were plated on 6 cm culture plates precoated with 0.2% gelatine (precoating of plates for at least 10 min; Sigma #G-1890) and cultivated in feeder medium. After grown to confluency feeder cells were inactivated by incubation in 1 mg/ml Mitomycin C (Sigma #M0503) for 2 hours. After washing three times with PBS (Invitrogen #3094370) ES medium was added. ES cells were plated on the feeder cell layer and splitted every other day to allow colonies to grow separately. Stem cells were splitted by washing once with PBS and incubation in 2.5 – 5ml trypsin/EDTA at 37°C until the cells detached from the plate. Cells were triturated in trypsin solution to obtain a single cell suspension and trypsin was finally inactivated by adding 5-7 ml of ES medium. Cells were centrifuged for 5 min at 1000 rpm and the pellet was resuspended in 5 ml ES medium. Cells were plated on freshly inactivated feeder cells. After three to four passages stem cells were plated on gelatine-coated 10 cm plates (Corning #430167) without feeder cells. Stem cells were splitted according to density and morphology every second day and the medium was replaced every other day. High proliferation was necessary for successful differentiation as well as it important that the cells were in a phase of rapid growth and formed a flat monolayer. Stem cells were either used for embryoid body formation immediately or frozen for later use.

Freezing of ES cells

For freezing, cells were trypsinized and centrifuged as for splitting. The pellet was resuspended in ES medium containing 10% DMSO (Dimethyl Sulfoxide; Sigma #D-4540) and the cell suspension was transferred into cryo tubes that were frozen in cryo boxes at -80°C. After 2-7 days the cryo vials were transferred to liquid nitrogen.

2.1.3 Embryoid body (EB) formation

EB medium

	concentration	supplier
FCS	10%	Invitrogen, personal reservation, heat inactivated 30 min at 55°C
non-essential amino acids (100x)	1x	Invitrogen #11140-035
glutamine (200 mM)	0.8 mM	Invitrogen #25030-024
β-mercaptoethanol	0.001%	Sigma #M7522
DMEM	to final volume	Invitrogen #21969-035

For EB formation stem cells were trypsinized according to the splitting protocol and resuspended in EB medium after centrifugation. Cells were counted either in a Neubauer counting chamber or with Casy® - 1 (Schärfe System GmbH, Reutlingen). The number of cells taken for EB formation was set individually for every ES cell line and was in the range of 1.5×10^6 to 4×10^6 ES cells. Cells were plated on bacterial dishes (Greiner bio-one #664160) in 15 ml EB medium.

The non-adhesive substrate of the bacterial dishes prevents attachment of the ES cells and free-floating three-dimensional structures, so-called embryoid bodies (EBs), are formed. EBs are kept in culture for 8 days in total. Every other day the medium was changed by putting the cell solution into a 50 ml falcon tube, letting the aggregates settle down for 4-5 min, removing the supernatant and resuspending EBs in fresh medium. After 4 and 6 days in culture, 5 μM retinoic acid (Sigma #R2625) was added to initiate neuronal differentiation.

2.1.4 Trypsinization of EBs

Coating of culture plates

0.5 mg/ml poly-DL-ornithine hydrobromide (Sigma #P8638) was dissolved in boric buffer (boric acid; Riedel-de Haën® #31146; pH8.4) and filtered. The solution was diluted 1:5 in aqua ad inject (Aichele Medico AG #530103) and culture plates (Nunc #150288) were coated in the incubator over night. After washing three times with aqua inject, laminin (Roche #11243217001) was added in a concentration of 0.5 µg/cm² in PBS for at least 2 hours.

N2 medium

	stock solution	final concentration	supplier
Insulin	5 mg/ml	25 µg/ml	Sigma #I-6634
Apo-Transferrin	2 mg/ml	50 µg/ml	Sigma #T-1147
Progesterone	20 µM	6 ng/ml	Sigma #P-8783
Putrescine	160 mg/ml	16 µg/ml	Sigma #P-5780
Sodium Selenite	300 µM	30 nM	Sigma #S-5261
BSA	10 mg/ml	50 µg/ml	Sigma #A-9418
DMEM & F12	mixed 1:1 to final volume		Invitrogen #21969-035 Invitrogen #21765-029

Complete medium

Medium was prepared according to Brewer et al. (1989) with the following chemicals omitted from the original protocol: glutamate, HEPES, corticosterone, lipoic acid, tri-iodothyronine.

aqueous solutions	stock solution	final solution	supplier
L-Alanin	2 mg/ml	2 µg/ml	Sigma #A-7627
Biotin	0.1 mg/ml	0.1 µg/ml	Sigma #B-4502

aqueous solutions	stock solution	final solution	supplier
L-Carnitine	2 mg/ml	2 µg/ml	Sigma #C-0283
Ethanolamine	1 mg/ml	1 µg/ml	Sigma #E-9508
D+ Galactose	15 mg/ml	15 µg/ml	Sigma #G-0625
L-Proline	7.76 mg/ml	7.76 µg/ml	Sigma #P-0380
Putrescine	16.1 mg/ml	16.1 µg/ml	Sigma #P-7505
Sodium-Selenite	0.016 mg/ml	0.016 µg/ml	Sigma #S-1382
Vitamine B12	0.34 mg/ml	0.34 µg/ml	Sigma #V-2876
Zinc sulfate	0.194 mg/ml	0.194 µg/ml	Sigma #Z-4750
Catalase	16 mg/ml	16 µg/ml	Sigma #C-40
Glutathione	1 mg/ml	1 µg/ml	Sigma #G-6013
SOD	2.5 mg/ml	2.5 µg/ml	Sigma #S-2515
ethanolic solutions			
Linoleic acid	100 mg/ml	1 µg/ml	Sigma #L-1376
Linolenic acid	100 mg/ml	1 µg/ml	Sigma #L-2376
Progesterone	0.63 mg/ml	6.3 ng/ml	Sigma #P-8783
all-trans-Retinol	10 mg/ml	100 ng/ml	Sigma #R-7632
Retinylacetate	10 mg/ml	100 ng/ml	Sigma #R-7882
Tocopherol	100 mg/ml	1 µg/ml	Sigma #T-3251
Tocopherolacetate	100 mg/ml	1 µg/ml	Sigma #T-3001

Stock solutions of each ingredient were stored at -20°C and used within 6 month.

For 400 ml complete medium, 1 g BSA (Sigma #A-9418), 2 mg transferrin (Sigma #T-1147) and 1.6 mg insulin (Sigma #I-6643) are dissolved in 30 ml DMEM and the remaining components are added, starting with the ethanolic solutions to dispose the foam. DMEM is added to final volume and medium is filtered and stored at 4°C for several weeks. Glutamine is added freshly before using the medium.

Dissociation procedure

EBs were collected in 50 ml falcon tubes and washed twice with PBS. 500 μ l freshly prepared trypsin/EDTA solution (0.05% trypsin in 0.04% EDTA/PBS; trypsin TPCK treated from bovine pancreas; Sigma #T-8802) was added to the EB pellet and incubated for 3 min at 37°C in the waterbath. The tube was gently shaken a few times. 10 ml EB medium were added to inactivate trypsin and EBs were dissociated by pipetting carefully up and down 5 to 6 times. Cell suspension was centrifuged for 5 min at 1000 rpm, the pellet was resuspended in 5 ml N₂ medium and the whole suspension was filtered through a cell strainer (BD Falcon™ #352340; 40 μ m pore size) to remove DNA and debris. Cells were counted and plated in a density between 4 and 5.5x10⁶ cells on PORN/Laminin-coated 6 cm plates and between 0.7x10⁶ and 1x10⁶ cells on PORN/laminin-coated 12 well plates. N₂ medium was replaced after 2 and 24 hours. After 48 hours the medium was exchanged to complete medium. Neurons were kept in complete medium for up to 3 weeks and medium was partially replaced during this time according to amount of debris.

After dissociation of EBs cells can also be frozen for later use. For this purpose cells were resuspended after centrifugation in EB medium with 10% DMSO (further processing see “freezing of ES cells”).

2.2 Immunostainings

Glass cover slips (Assistant, microscopical cover glasses, #1001/18) were prepared by incubating them in 65% nitric acid (Riedel-de Haën® #32213) for 1-2 d. After rinsing them with H₂O for several hours they were floated in ethanol, air-dried and sterilized under UV light. Neurons grown on PORN/Laminin-coated cover slips were washed once with PBS and fixed with 4% paraformaldehyde (PFA, prewarmed to 37°C; Merck #1.04005.1000) for 10 min, washed three times with PBS and either kept in PBS at 4°C until further processing or used immediately for immunostainings.

Immunostainings were performed by blocking the cells for 1 h at room temperature (RT) in blocking buffer (10% normal goat serum (Sigma #G-9023), 0.03% Carrageenan (Sigma #C-1138) and 0.3% Triton®X-100 (Fluka #93426)). Primary antibody was added in 2% NGS, 0.03% Carrageenan and 0.3%Triton at 4°C over night. After washing three times with PBS the secondary antibody was added in

the same buffer for 1 hour at RT. DAPI (4',6'-diamidino-2-phenylindole; 1:10000; AppliChem #28718-90-3) was added following the secondary antibody treatment, for 3 min. Cover slips were washed three times with PBS before mounting in Aqua Poly Mount (Polyscience Incorporated #18606) on an object slide. Immunostained cover slips were stored in the dark at 4°C (for details about antibodies used see Table I).

2.3 Glutamate Release Assay

HANKs buffer

	concentration	supplier
NaCl	125 mM	Fluka #71381
KCl	5 mM	Fluka #60132
NaH ₂ PO ₄ ·2H ₂ O	1.2 mM	Fluka #71500
CaCl ₂	1 mM	Sigma #C-5080
MgCl ₂	1.2 mM	Sigma #M-2670
ZnCl ₂	1 μM	Sigma #Z-0152
Glucose	10 mM	Sigma #G-5400
HEPES	25 mM	Sigma #H-6147
BSA	0.25 %	Sigma #A-9418

Glutamate release assay was performed as described in Griesbeck et al., 1999, with slight modifications. In brief, neurons on 12 well plates derived from wild-type and *app*^{-/-} *aplp2*^{-/-} stem cells were kept in culture for 14 days. All cells were incubated with 1 μl ³[H]-Glutamate (L-[G-3H] Glutamic acid 9.25 MBq, Amersham Bioscience #3-4900220929) for 1 hour at 37°C. After washing cells twice with HANKs buffer (prewarmed at 37°C), medium was collected every 5 min and replaced by fresh medium. After 25 min (= 6th fraction) and 45 min (=10th fraction) 50 mM KCl or 100 μM glutamate was added. The medium was collected until fraction 12 and the amount of ³[H] was determined by a scintillation counter.

Data analysis was performed using Excel program. To quantify the amount of glutamate being released by either cell line, the mean value of fractions 4 and 5 before the stimulation (a) and the mean value of fractions 7 and 8 after the stimulation (b) event were taken and the mean was calculated $((a + b)/2)$. This mean value was subtracted from the value of fraction 6 (c) which displays the amount of glutamate released directly after stimulation. The mean of the values from each single experiment was calculated, as well as the standard deviation and standard deviation of the mean.

2.4 Western Blot

Lysis buffer

	concentration	supplier
Trizma [®] base	50 mM	Sigma #T-6791
NaCl	150 mM	Fluka #71381
Triton [®] X-100	1%	Fluka #93426
Glycerine (87%)	10%	Merck #1.04094.1000

Protease inhibitors were freshly added to the lysis buffer (protease inhibitor cocktail tablets, Roche #11836153001).

After washing cells twice with cold PBS, cell extracts were prepared by adding lysis buffer (750 μ l for a 6 cm plate; 300 μ l for a well from a 12 well plate). Cells were rinsed with the lysis buffer until they detached and the solution was triturated. After centrifugation (4200 rpm, 30 min, 4°C) supernatant was collected and aliquots were stored at -80°C until further use.

Western Blots were performed with the NuPAGE[®] System from Invitrogen. If not stated differently, all reagents and materials were purchased from Invitrogen.

For 20 μ l of sample, 5 μ l NuPAGE LDS sample buffer (# NP0007), 2 μ l NuPAGE reducing agent (# NP0004) and x μ l sample were prepared. Samples were heated for 10 min at 70°C and loaded onto a gel. Volumes loaded were adjusted such that the expression of proteins taken for normalization purpose

were similar (~1.5 µl of 750 µl total protein extract). A protein marker interacting with the secondary antibody was used (MagicMark™XP Western Protein Standards #LC5602). The Western transfer was performed using the XCell II™ Blot Module on PVDF membranes (# LC2005).

Washing buffer (TBST, 0.2% Tween)

	concentration	supplier
NaCl	137 mM	Fluka #71381
KCl	2.7 mM	Fluka #60132
Trizma® base	25 mM	Sigma #T-6791
Tween® 20	0.2%	Sigma #P-1379

The membrane was blocked with 5% milk powder in washing buffer for 1 hour on a shaker at room temperature. The primary antibody was added to the membrane in 2% milk powder in washing buffer and incubated at 4°C on a shaker over night. After washing several times the secondary antibody was added in 2% milk powder in washing buffer and incubated for 1-1.5 hours at room temperature. Subsequently, the membrane was washed in washing buffer, incubated with chemiluminescence detection solution (ECL plus, Amersham Bioscience #25006277) and exposed to Hyperfilm ECL (Amersham Bioscience #25800095).

2.5 RT-PCR

2.5.1 RNA isolation

Isolation of RNA was based on the protocol of Chomczynski et al., 1987.

After washing cells twice with cold PBS, they were lysed by adding TRIZOL® Reagent (Invitrogen #15596-018; 1 ml for a 6 cm plate, 300 µl for one well from a 12 well plate). 0.1 ml chloroform (Sigma #C-2432) per ml TRIZOL® was added and the sample was vigorously vortexed and incubated on an Eppendorf shaker (10 min, 400 rpm). The homogenate was centrifuged (10 min, 14000 rpm, RT) and

the upper aqueous phase containing the extracted RNA was transferred to a fresh tube. An equal volume of cold isopropanol (Fluka #59310) was added and the solution was incubated for 10 min on ice. Precipitated RNA was collected by centrifugation for 10 min at 14000 rpm. After washing the RNA pellet once with 70% ethanol (Fluka #02883) RNA was dried and dissolved in 10 mM Tris (pH 7.5). The RNA solution was either stored at -80°C or further processed immediately. To remove traces of DNA, the RNA solution was incubated with 5 mM MgCl₂ and 10 units DNase (Roche #776 785) for 1h at 37°C. To remove DNase, phenol/chloroform extraction was performed by adding 1 volume H₂O and 1 volume phenol:chloroform:isoamyl alcohol 25:24:1 (Sigma #P-3803). The solution was vortexed and centrifuged for 5 min at 14000 rpm. The upper phase was collected and 0.3 M sodium acetate (NaAc, pH 5.2) and 3 volumes ethanol were added for DNA precipitation. The solution was incubated for 10 min on ice and centrifuged for 25 min at 14000 rpm at 4°C. After washing the RNA pellet once with 70% ethanol, pellet was dried and dissolved in 10 mM Tris (pH 7.5). RNA was quantified using the ND-1000 machine (NanoDrop Technologies) and aliquots of 400 ng RNA were stored at -80°C.

2.5.2 cDNA Synthesis

For first-strand cDNA synthesis 400 ng of DNase-treated total RNA were mixed with 300 ng random primers (Invitrogen #48190-011). To perform primer annealing the solution was incubated at 65°C for 5 min and slowly cooled down to 25°C (0.1°C/sec). Reverse transcriptase reaction was carried out with 50 units reverse transcriptase (RT, Stratagene #600085), 0.5 mM dNTPs (Invitrogen #10297-117) and 50 mM Tris-HCl, 75 mM KCl and 3mM MgCl₂ (Stratagene #600085-52) in a final volume of 50 µl. The mixture was incubated for 1 h at 42°C and reverse transcriptase was inactivated for 5 min at 90°C. The cDNA synthesized as described has a concentration of 8 ng/µl and was diluted to a final concentration of 1 ng/µl and stored at -20°C until further use.

2.5.3 Semi-quantitative RT-PCR

PCR Master Mix for 50 μ l reaction volume:

	concentration	supplier
PCR buffer (-MgCl ₂)	20 mM Tris-HCl; 50 mM KCl	Invitrogen #18038-026
dNTP	200 nM	Invitrogen #10297-117
MgCl ₂ (50 mM)	1.5 mM	Invitrogen #18038-026
forward primer	200 nM	Microsynth
reverse primer	200 nM	Microsynth
Taq Polymerase	2 units	Invitrogen #18038-026
cDNA	1 μ l	

For primer sequences see Table II.

PCR amplification protocol:

step 1: 95°C	5 min
step 2: 95°C	1 min
step 3: 63°C	1 min
step 4: 72°C	1 min
step 5: 72°C	2 min

Steps 2-4 were repeated 34 times.

PCR products and 1 kb ladder (US Biological, #03930-11A) were loaded on a 1.5 % agarose (Invitrogen #15510-027) gel containing 0.5 μ g/ml ethidiumbromide (Sigma #E1510). Gel detection was performed with Vilber Lourmat gel detection system, a CHOU high performance CCD camera and print outs were done with a SONY video graphic printer UP-890 CE.

2.5.4 Quantitative RT-PCR

Quantitative RT-PCR was performed using TaqMan[®] probes. The primers were double-dye oligonucleotides with FAM as the fluorescent reporter dye at the 5' end and TAMRA as the quencher dye at the 3' end. Inventoried assays for detection of *vglut2* and *synaptophysin* transcription were purchased from Applied Biosystems (see Table III). Primers and probes for *tau*, *egfp*, human *APP* (hAPP) and mouse *app* (ms *app*) detection were designed using primer express software from ABI according to manufacturers advices and bioinformatic analysis to isolate specific amplicon sequences. They were purchased from Microsynth.

From each RNA sample two to three independent cDNAs were synthesized. With each cDNA two to three independent PCRs were performed, using every sample in triplicates.

The following master mixes were prepared for individual genes:

18S transcription

	concentration	supplier denotation
2xQPC PCR master mix probe assay	1x	qPCR Master Mix, RT-QP2X-03; Eurogentec
18S primer mix (10 μ M)	300 nM	RT-CKFT-18S; Eurogentec
18S FAM-TAMRA probe (6.25 μ M)	175 nM	

vglut2 or *synaptophysin* transcription

	concentration	supplier denotation
2xQPC PCR master mix probe assay	1x	qPCR Master Mix, RT-QP2X-03; Eurogentec
FAM-TAMRA primer mix and probe (20x)	1x	Mm 00499876_m1 (<i>vglut2</i>); Mm 00436850_m1 (<i>synaptophysin</i>); ABI Applied Biosystems

***tau*, *hAPP*, *ms app* or *egfp* transcription**

	concentration	supplier denotation
2xQPC PCR master mix probe assay	1x	qPCR Master Mix, RT-QP2X-03; Eurogentec
Primer 1 (10 μ M)	300 nM	Microsynth
Primer 2 (10 μ M)	300 nM	
FAM-TAMRA probe (0.175 μ M)	175 nM	

Per 20 μ l reaction volume 5 ng cDNA were taken. Quantitative RT-PCR was performed in 96-well plate format with an ABI Prism[®] SDS 7900 HT thermocycler. Minus RT controls were included to check for traces of genomic DNA as well as non-template controls to check for primer dimerization.

PCR amplification protocol:

step 1: 50°C	2 min
step 2: 95°C	10 min
step 3: 95°C	15 seconds
step 4: 60°C	1 min

Step 3-4 were repeated 39 times.

2.6 Genotyping

tail buffer

	concentration	supplier
Trizma hydrochloride	100 mM (pH8.5)	Sigma #T-3253
EDTA	5 mM	Sigma #E-5134
NaCl	200 mM	Fluka #71381
SDS	0.2 %	Sigma #L-4390

Mouse tails were incubated in tail buffer containing 0.1 µg/µl Proteinase K (Merck #1.24568.0500) on an Eppendorf shaker (400 rpm, 55°C over night). The solution was centrifuged (14000 rpm, 1 min) and the supernatant was transferred into 500 µl isopropanol. The solution was centrifuged (14000 rpm, 30 min) and the pellet was washed once with 70% Ethanol. DNA was subsequently dried and resuspended in 300 µl TE (pH 8). DNA was resuspended by agitation at 55°C over night before performing the PCR.

PCR Master Mix for 50 µl reaction volume:

	concentration	supplier
PCR buffer (-MgCl ₂)	20 mM Tris-HCl; 50 mM KCl	Invitrogen #18038-026
dNTP	200 nM	Invitrogen #10297-117
MgCl ₂ (50 mM)	1.5 mM	Invitrogen #18038-026
forward primer 1	200 nM	Microsynth
forward primer 2	200 nM	Microsynth
reverse primer	200 nM	Microsynth
Taq Polymerase	2 units	Invitrogen #18038-026
DNA	1µl	

Primer pair UM42 (for sequence see Table IV) and UM44 detect the app wild-type allele (650 bp length); primer pair UM42 and P3-hygro detect the targeted allele (430 bp length). Primers aplp2-1 and aplp2-2 detect the aplp2 wild-type allele (400 bp length) and primer pair aplp2-1 and aplp2-3 detect the targeted allele (350 bp).

PCR amplification protocol for genotyping:

step 1: 95°C	2 min
step 2: 95°C	30 sec
step 3: 63°C	30 sec
step 4: 72°C	30 sec
step 5: 72°C	5 min

Step 2-4 were repeated 34 times.

PCR products were loaded on 1.5 % agarose gels and run at 150 Volt. For detection see semi-quantitative RT-PCR.

Table I

Primary antibodies

	source	dilution	supplier
APLP1 (β -amyloid precursor-like protein1), C-terminal	rabbit	1:3000 (Western)	Calbiochem #171615
APLP2 (β -amyloid precursor-like protein2), C-terminal	rabbit	1:5000 (Western)	Calbiochem #171616
APP C8 (amyloid- β -precursor protein), C-terminal	rabbit	1:3000 (Western)	P. Paganetti, personal gift
human amyloid- β protein (clone: 6E10)	mouse	1:2000 (Western)	Signet Laboratories #9300-02
EGFP	rabbit	1:1000 (Western)	BD Biosciences #8367-2
GluR1	rabbit	1:1000 (Western)	Upstate, #06-306
rat-401, nestin	mouse	1:10 (Immunocytochemistry)	Developmental Studies Hybridoma Bank
Pax6	mouse	1:100 (Immunocytochemistry)	Developmental Studies Hybridoma Bank
PSD-95 (post synaptic density protein-95)	mouse	1: 1000 (Western)	Sigma #P-246
RC2	mouse	1:4 (Immunocytochemistry)	Developmental Studies Hybridoma Bank
synaptobrevin/VAMP2	mouse	1:10000 (Western)	Synaptic Systems SySy #104 201
synaptophysin	mouse	1:2000 (Western)	Sigma #S-5768
tau-1	mouse	1: 3000 (Western)	Chemicon International #MAB3420
β -tubulin isotype III	mouse	1:5000 (Western)	Sigma #T-8660
VGLUT1 (BNPI, vesicular glutamate transporter1)	mouse	1:3000 (Western)	Chemicon International #MAB5502
VGLUT2 (DNPI, vesicular glutamate transporter2)	rabbit	1:5000 (Western)	Synaptic Systems SySy #135 102

Secondary antibodies

Cy TM 3-conjugated AffiniPure Goat Anti-Mouse IgG (H+L)	1:500	Jackson ImmunoResearch #115-165-062
Cy TM 3-conjugated AffiniPure Goat Anti-Rabbit IgG (H+L)	1:500	Jackson Immuno Research #111-165-144
Peroxidase conjugated AffiniPure Goat Anti-Mouse IgG (H+L)	1:10000	Jackson Immuno Research #115-035-062
Peroxidase conjugated AffiniPure Mouse Anti-Rabbit IgG (H+L)	1:5000 1:10000	Jackson Immuno Research #211-035-109

Table II

Primers for semi-quantitative RT-PCR (all sequences are written 5' → 3')

	forward primer	reverse primer
<i>apl1</i>	GTGAAGAAACGTGGGATGGTG	GAACTGGACGCCTCTGTGC
<i>apl2</i>	GCCACCGGCAAGCTTCTTG	CAGCGCTGGTGCTTCTCAC
<i>tau</i>	CCTCTTCTGTCCTCGCCTTCG	CTTCGTTCTCCGGATTTTGGTG
<i>vglut2</i>	CTG TCG GGG ATG GTT TGC	CGGCATAACGTGACAACACTGC

Table III

Primers for quantitative RT-PCR (all sequences are written 5' → 3')

	forward primer	reverse primer	targeted region
18S RNA	unknown	unknown	unknown
hAPP (tau-happ fusion cDNA)	CCTCTTCTGTCCTC GCCTTCTG	TAGCCCCCCTGAT CTTTC CT	cgaTTATCAGGGTtta aacegccaccatggt
<i>ms app</i>	CCCTGGTGATGTT GAAGAAGAAA	TCTGCTGCATCTTG GAGAGATG	CGGCGTCGACCTC CACCACG

	forward primer	reverse primer	targeted region
<i>egfp</i>	CCAGGAGCGCACC ATCTT	CGATGCCCTTCAG CTCGAT	CTACAAGACCCGC GCCGAGGTGA
<i>tau</i>	GGGCAGCATCGAC ATGGT	TGGCCAAGGAAGC AACAT	CACCACAGCTTGC CACACTAGCCGAT
<i>synaptophysin</i>	unknown	unknown	NM_009305, exon2- exon3, probe in 82
<i>vglut2</i>	unknown	unknown	NM_080853, exon8- exon9, probe in 1609

Table VI

Primers for genotyping (all sequences are written 5' → 3')

	forward primer	reverse primer
UM42 short= primer 3'		CACCTGGTTCTAATCAGA GGC
UM44 short = primer 5'	GAGACGAGGACGCTCAGTC CTAG	
P3-hygro short = primer 5' in the inserted PGK-polyA part	CGAGATCAGCAGCCTCTGT C	
aplp2-1	GCCAAGCTTGAGTCGGTGT ATCCGTGCT	
aplp2-2		GCGACCGGAGGAGACGCA GATCGGGAGCTCGCC
aplp2-3	CCATTGCTCAGCGGTGCTG	

Results

3.1 Isolation and characterization of embryonic stem cells lacking *app* or *app* and *aplp2*

3.1.1 Isolation and characterization of ES cells from *app*^{-/-} and *app*^{-/-} *aplp2*^{-/-} mice

Mouse embryonic stem (ES) cell lines lacking APP or APP and APLP2 were isolated from *app*^{-/-} and *app*^{-/-} *aplp2*^{-/-} blastocysts which were derived from *app*^{-/-} and *app*^{-/-} *aplp2*^{-/-} mice, kindly provided by Prof. U. Müller (MPI für Hirnforschung, Frankfurt/M.; Heber et al., 2000).

App^{-/-} males (genetic background of 129OLAxC57BL/6) were backcrossed with SV129 Paslco females for one generation to obtain heterozygote animals. Subsequent crossing of the heterozygote animals generated blastocysts from all three genotypes (*app*^{+/+}, *app*^{+/-}, *app*^{-/-}) allowing the isolation of different ES cell lines with the same genetic background. In addition, backcrossing with Sv129 lines increases the isolation efficiency. Indeed, most of the commonly used ES cell lines are derived from strain 129 (Evans et al., 1981).

As *app*^{-/-} *aplp2*^{-/-} mice (genetic background of 129Sv(ev)xC57BL/6) are postnatally lethal, *app*^{+/-} *aplp2*^{-/-} animals were crossed to obtain blastocysts with the desired *app*^{-/-} *aplp2*^{-/-} genotype for ES cell isolation.

Embryonic stem cells were isolated from the inner cell mass (ICM) of blastocysts (Robertson, 1987). Females were injected with pregnant mare's serum (PMS, 5 U/animal) and two days later with human chorionic gonadotropin (hCG, 5 U/animal) for super-ovulation. Matings were set up directly after the last injection (referred to as day 0) and plaques were checked after 4 hours and the next morning. At day 3.5 post coitum (pc) blastocysts were collected and plated on mouse embryonic feeder cells (MEFs). At day 6.5 pc ICMs were picked, dissociated and plated on new MEFs. ES cell clones were

picked between 10.5 and 16.5 days pc. ES cell lines were passaged every second day on MEFs and cells were frozen after the second and third passage. For further characterization ES cells were kept in culture without feeder cells for up to three passages and genotype (see Materials and Methods; Fig. 2 and Fig. 3) as well as karyotype were determined. Also, the presence of mycoplasma was checked.

For the present work three ES cell lines were used:

- clone 159-2 (wild-type), derived from *app*^{+/-} crossings
- clone 149-1 (*app*^{-/-}), derived from *app*^{+/-} crossings
- clone B8-1 (*app*^{-/-} *aplp2*^{-/-}), derived from *app*^{+/-} *aplp2*^{-/-} crossings.

All three ES cell lines were male, harbor 40 chromosomes and were negative for mycoplasma.

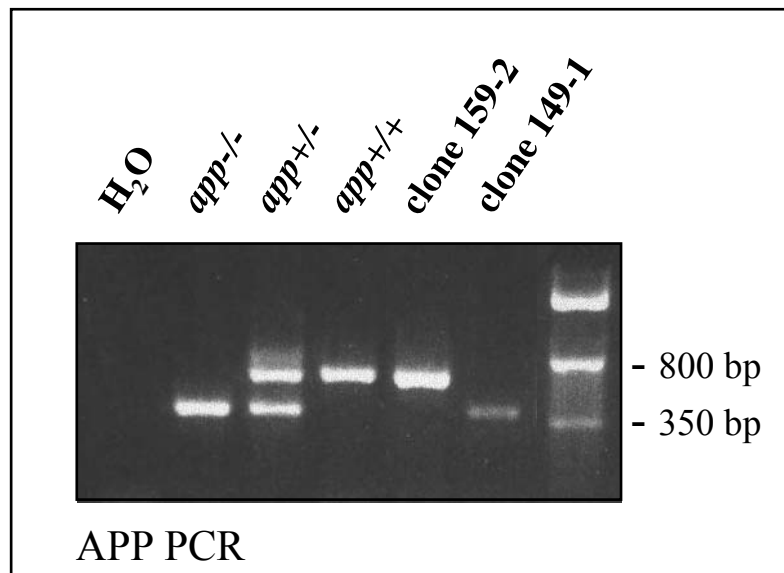


Figure 2: Genotyping of the wild-type and *app*^{-/-} ES cell clones

Genotyping of ES cells was performed after the cells had been in culture for several passages without MEFs (see Materials and Methods for primer sequences and protocol). Primers for *app* gene detection amplify a wild-type (*app*^{+/+}) fragment of 650 bp length and a knock-out (*app*^{-/-}) fragment of 430 bp length. Clone 159-2 shows a wild-type fragment and is characterized as wild-type ES cell line (*app*^{+/+} ES cell line). Clone 149-1 shows a knock-out fragment and therefore lacks the *app* gene (*app*^{-/-} ES cell line).

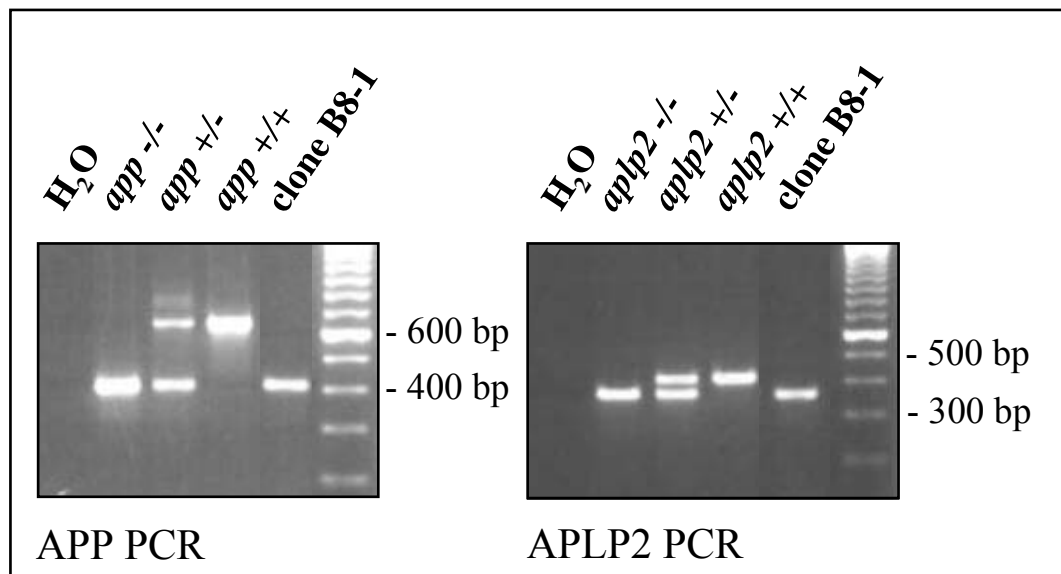


Figure 3: Genotyping of the *app*^{-/-} *apl2*^{-/-} ES cell clone

Genotyping of ES cells was performed after the cells had been in culture for several passages without MEFs (see Materials and Methods for primer sequences and protocol). Primers for *app* gene detection amplify a wild-type (*app*^{+/+}) fragment of 650 bp length and a knock-out (*app*^{-/-}) fragment of 430 bp length. Primers for *apl2* gene detection amplify a wild-type (*apl2*^{+/+}) fragment of 400 bp length and a knock-out (*apl2*^{-/-}) fragment of 350 bp length. Clone B8-1 shows fragments referring to *app*^{-/-} and *apl2*^{-/-} and therefore lacks the *app* and *apl2* gene (*app*^{-/-} *apl2*^{-/-} ES cell line).

3.1.2 Characterization of neurons derived from *app*^{-/-} and *app*^{-/-} *apl2*^{-/-} ES cells

The embryonic stem cell clones 159-2 (wild-type), 149-1 (*app*^{-/-}) and B8-1 (*app*^{-/-} *apl2*^{-/-}) were differentiated into neurons according to the protocol of Bibel et al., 2004 (further details see Materials and Methods).

The absence of APP or APP and APLP2 in neurons derived from *app*^{-/-} and *app*^{-/-} *apl2*^{-/-} ES cells was confirmed by Western Blot analysis (Fig. 4 – Fig. 6). Protein extracts from neurons were taken 3, 5, 6, 8, 9, 10 and 12 days after dissociation of EBs (referred to as 3, 5, 6, 8, 9, 10 and 12 days *in vitro*, DIV) and equal protein volumes were loaded onto the gel. Expression of APP was tested with an antibody raised against the 19 C-terminal amino acids of human APP (APP C8 personal gift P. Paganetti, Novartis) that cross-reacts with mouse APP. Also, due to the high sequence homology between the three APP family proteins, this antibody might cross-react with APLP1 and APLP2.

APP could not be detected in neurons derived from *app*^{-/-} and *app*^{-/-} *apl2*^{-/-} ES cells. In wild-type neurons, expression of APP increases during the course of neuronal differentiation (Fig. 4).

APLP1 protein expression was found in neurons of all three cell lines (Fig. 5) while APLP2 protein was

shown to be absent in *app*^{-/-} *aplp2*^{-/-} neurons but present in wild-type and *app*^{-/-} neurons. Its expression increases during the course of differentiation (Fig. 6).

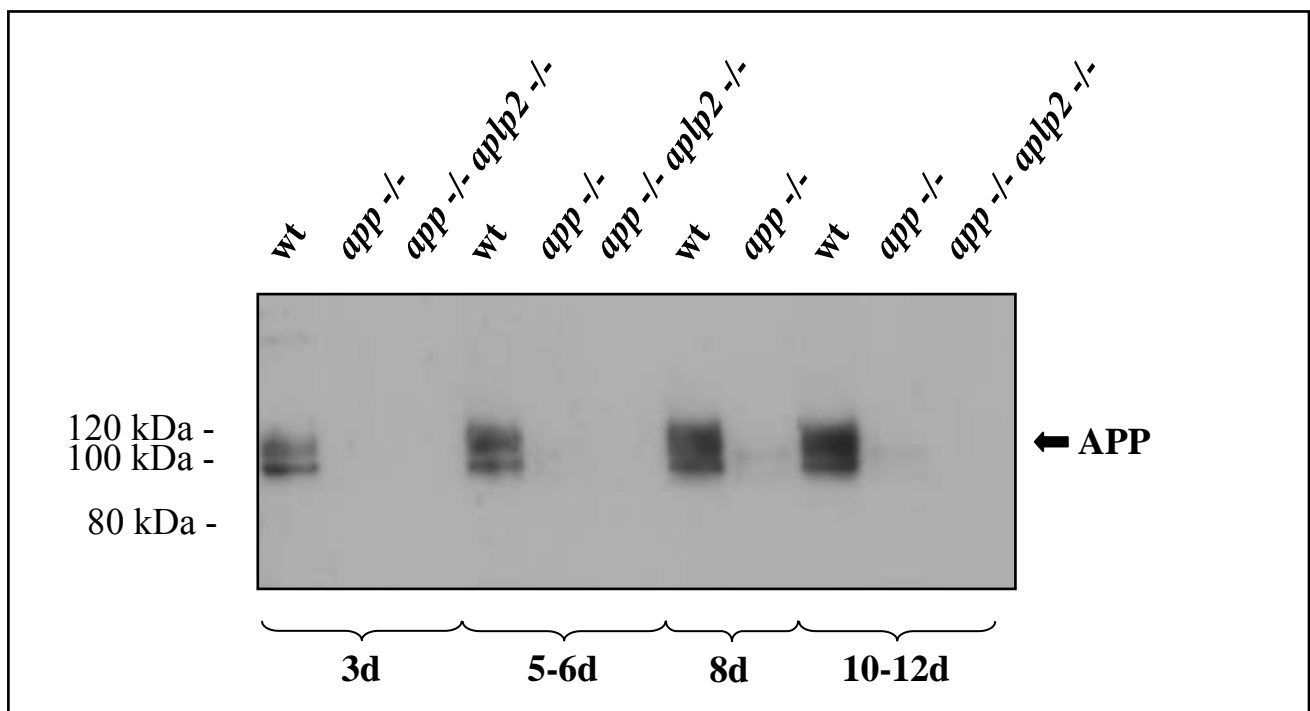


Figure 4: Expression of APP protein in neurons derived from ES cells

Western Blots were performed with protein extracts of wild-type, *app*^{-/-} and *app*^{-/-} *aplp2*^{-/-} neurons lysed after 3, 5, 6, 8, 9, 10 and 12 days *in vitro* (d). Equal volumes of protein extracts were loaded on a 7% Tris- Acetate gel and separated by SDS-PAGE. After protein transfer membrane was probed with a polyclonal APP antibody that recognizes human and mouse APP protein (APP C8) (for antibody dilution and further details see Materials and Methods). APP protein was detected between 100-120 kDa and showed increasing levels over time in wild-type neurons but was absent in *app*^{-/-} and *app*^{-/-} *aplp2*^{-/-} neurons.

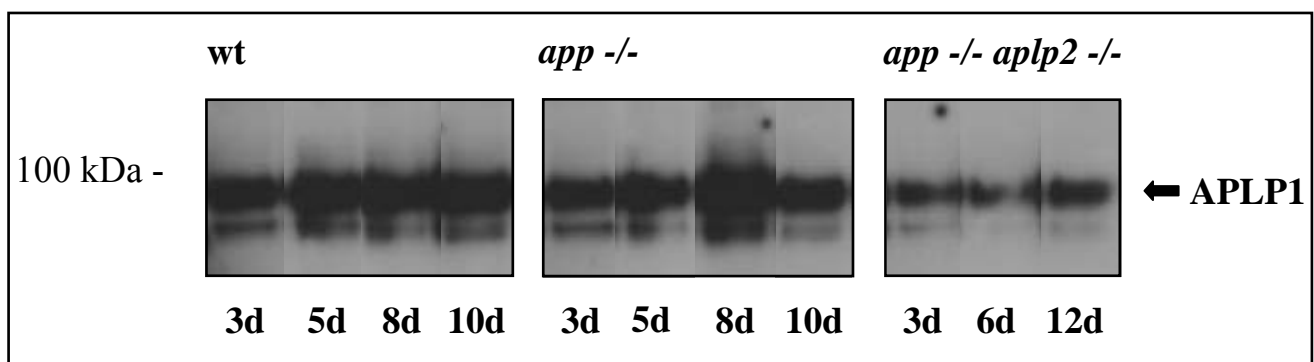


Figure 5: Expression of APLP1 protein in neurons derived from ES cells

Western Blots were performed with protein extracts of wild-type, *app*^{-/-} and *app*^{-/-} *aplp2*^{-/-} neurons lysed after 3, 5, 6, 8, 9, 10 and 12 days *in vitro* (d). Equal volumes of protein extracts were loaded on a 7% Tris-Acetate gel and separated by SDS-PAGE. After protein transfer membrane was probed with a polyclonal APLP1 antibody that recognizes the C-terminus of mouse APLP1 protein (for antibody dilution and further details see Materials and Methods). APLP1 protein was detected at 95 kDa and was present in neurons derived from all three ES cell lines.

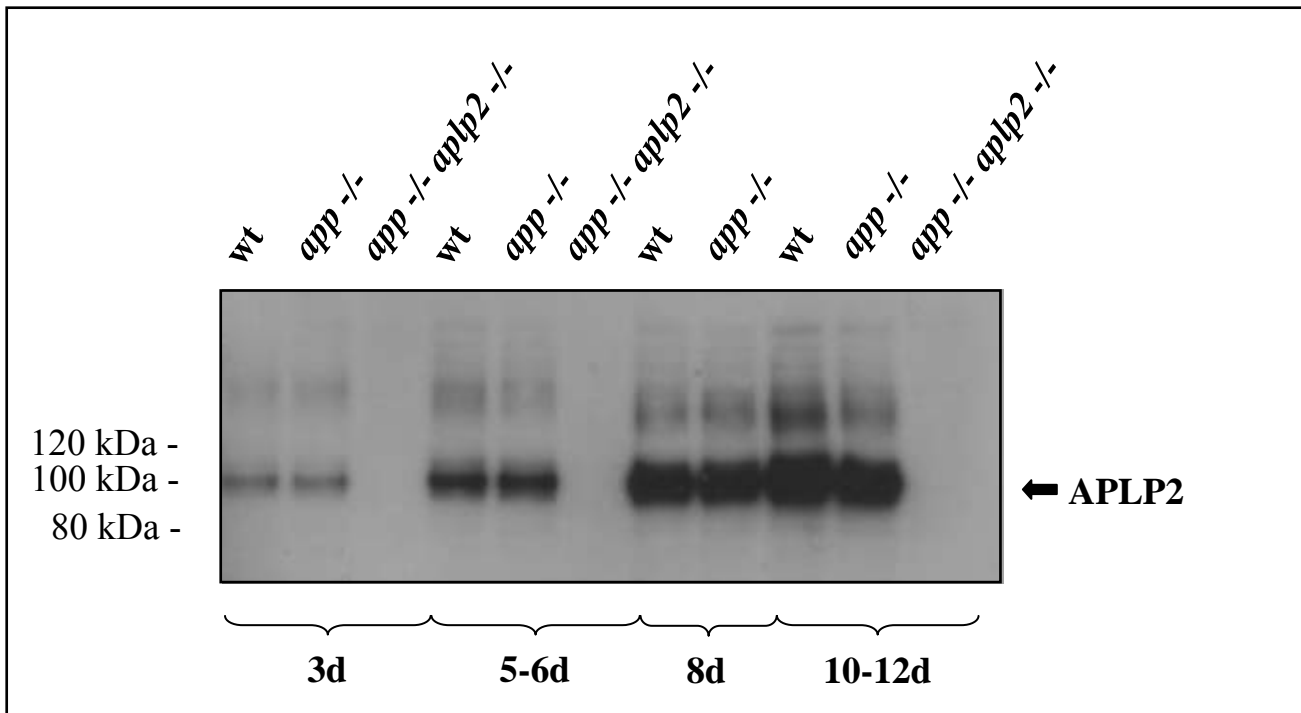


Figure 6: Expression of APLP2 protein in neurons derived from ES cells

Western Blots were performed with protein extracts of wild-type, *app*^{-/-} and *app*^{-/-} *aplp2*^{-/-} neurons lysed after 3, 5, 6, 8, 9, 10 and 12 days *in vitro* (d). Equal volumes of protein extracts were loaded on a 7% Tris-Acetate gel and separated by SDS-PAGE. After protein transfer membrane was probed with a polyclonal APLP2 antibody that recognizes the C-terminus of mouse APLP2 protein (for antibody dilution and further details see Materials and Methods). APLP2 protein was detected ~110 kDa and was not present in neurons derived from *app*^{-/-} *aplp2*^{-/-} cells while wild-type and *app*^{-/-} neurons show increasing levels of APLP2 expression during course of differentiation.

We tested by Western blot and semi-quantitative RT-PCR if a compensatory upregulation of *aplp1* occurs in the absence of *app* and *aplp2*. Western Blot and RT-PCR were performed with protein and RNA extracts respectively, isolated from 12 days old neurons. The volumes of protein extracts were normalized to volumes representing equal amounts of tau. APLP1 protein and RNA levels did not change in the absence of *app* and *aplp2* (Fig. 7 and Fig. 8). As a result of some variation in the quality of independent differentiations, differences in protein levels within one genotype were occasionally observed (note for example variations of APLP1 levels in the two independent wild-type differentiations shown in Fig. 7).

These results show that APP and APLP2 were absent in neurons derived from ES cells lacking both genes. APLP1 expression was detectable, but it did not show a compensatory upregulation in the absence of the two other APP family members.

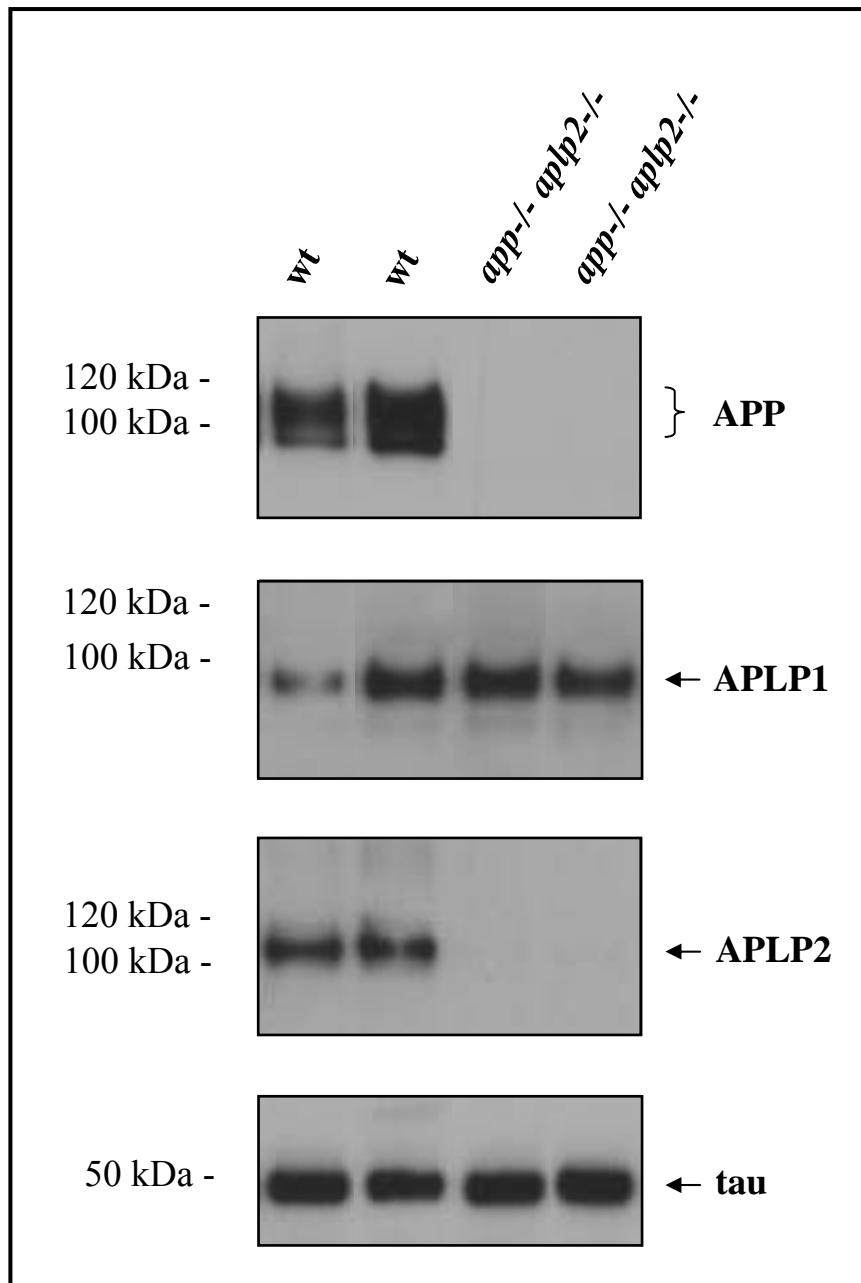


Figure 7: Expression of APP, APLP1 and APLP2 protein in neurons after 12 DIV

Western Blots were performed with protein extracts from two independent differentiations of either genotype. Extracts were taken from wild-type and *app*^{-/-} *apl2*^{-/-} neurons after 12 DIV and the volumes of loaded protein extract were normalized to volumes representing equal amounts of tau protein. Protein extracts were loaded on 7% Tris-Acetate gels for detection of APP and APP-related proteins and on a 10% Bis-Tris gel for detection of tau protein. Protein separation was performed by SDS-PAGE and after protein transfer membranes were probed with antibodies recognizing tau (tau-1), APP (APP C8), APLP1 or APLP2 (for further details see Materials and Methods). Tau protein was detected at 50 kDa, APP between 100-120 kDa, APLP1 at 95 kDa and APLP2 at 110 kDa. APLP1 showed no upregulation in *app*^{-/-} *apl2*^{-/-} neurons compared to wild-type neurons.

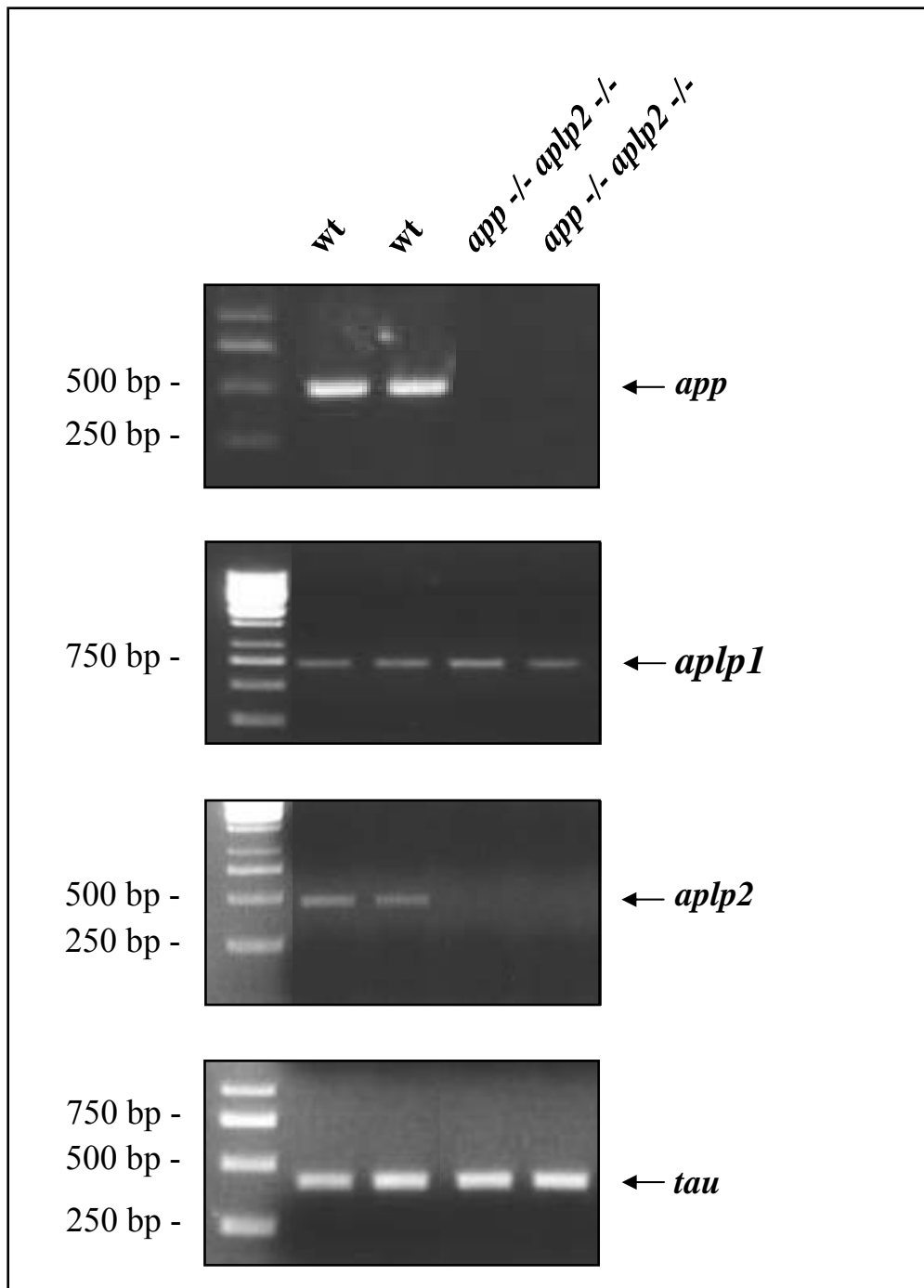


Figure 8: Analysis of APP, APLP1 and APLP2 transcripts

Semi-quantitative RT-PCR was performed with RNA extracts from two independent differentiations of either genotype. RNA was isolated from wild-type, *app*^{-/-} and *app*^{-/-} *aplp2*^{-/-} neurons after 12 DIV and cDNA synthesized according to standard protocol (for details see Materials and Methods). Primers used for *app* detection amplify a fragment of 450 bp length, primers used for *aplp1* detection amplify a fragment of 750 bp length and primers used for *aplp2* detection amplify a fragment of 464 bp length. *Tau* was used as housekeeping gene and primers for its detection amplify a fragment of 422 bp length. Note that the levels of *aplp1* appear to be similar in both genotypes.

3.2 Characterization of neural progenitors derived from ES cells lacking *app* or *app* and *aplp2*

Neuronal differentiation of ES cells according to our protocol results in an essentially homogenous population of neural progenitors with all the characteristics of radial glial cells. In addition, these cells express the transcription factor Pax6 (Bibel et al., 2004). Recently, Pax6-positive radial glial cells in the developing telencephalon have been found to generate virtually all pyramidal neurons in the developing cortex (Malatesta et al., 2003). Likewise, the differentiation of radial glial cells in our system results in the generation of glutamatergic neurons (Bibel et al., 2004). These neurons show characteristics comparable to those found in the cerebral cortex or hippocampus, as revealed by electrophysiological and biochemical criteria.

In addition to the expression of typical radial glial cell markers such as nestin and RC2, APP has been shown to be highly expressed in radial glial cells *in vivo* (Trapp et al., 1994). In line with this, we found that our ES cell derived radial glial cells also express high levels of APP (Bibel et al., 2004).

To investigate whether deletion of *app* or *app* and *aplp2* would influence the generation of radial glial cells and their subsequent differentiation in neurons, we characterized the neural progenitors derived from ES cells lacking *app* or *app* and *aplp2* for the presence of nestin, RC2 and Pax6.

We found that the neural progenitors generated from wild-type and knock-out ES cells show a similar morphology. We fixed the cells 2-5 and 24 hours (h) after dissociation of EBs and quantified the proportion of cells expressing the markers nestin, RC2 and Pax6 in relation to the total number of cells assessed by DAPI- (4',6'-diamidino-2-phenylindole) staining. Nestin immunostaining resulted in $87.8 \pm 7.6\%$ positive *app*^{-/-} and $91.2 \pm 6.8\%$ positive *app*^{-/-} *aplp2*^{-/-} cells after 2-5 h compared to $92.1 \pm 8.8\%$ of positive cells in the wild-type and its expression decreased to $49.6 \pm 7\%$ in *app*^{-/-} and $40 \pm 12.8\%$ in *app*^{-/-} *aplp2*^{-/-} cells and $60.5 \pm 14.8\%$ in the wild-type after 24 h (Fig. 9). After 2-5 h $100 \pm 0\%$ of *app*^{-/-} and $97.1 \pm 3.9\%$ of *app*^{-/-} *aplp2*^{-/-} cells were RC2-positive compared to $100 \pm 0\%$ positive cells in the wild-type. $98.9 \pm 1.9\%$ of *app*^{-/-} and $88.7 \pm 12.2\%$ of *app*^{-/-} *aplp2*^{-/-} cells were still positive after 24 h and $100 \pm 0\%$ of the wild-type neurons (Fig. 10). 2-5 h after plating $85.9 \pm 7.3\%$ of *app*^{-/-} and $88.1 \pm 6\%$ of *app*^{-/-} *aplp2*^{-/-} cells were Pax6-positive compared to $93.4 \pm 6.6\%$ of the wild-type cells. Its expression after 24 h decreased to $60 \pm 3.2\%$ in *app*^{-/-} and $59.4 \pm 18.3\%$ in *app*^{-/-} *aplp2*^{-/-} cells compared to $58.5 \pm 10.9\%$ in the wild-type (Fig. 11 and Fig. 12).

These results indicate that the absence of *app* or *app* and *aplp2* plays no role with regard to the generation of Pax6-positive radial glial cells. Like wild-type cells, the mutant progenitors display similar antigenic characteristics. Irrespective of their genotype, they subsequently all differentiate into neurons, as judged by expression of neuron specific markers such as β -tubulin and synaptophysin (Chapter 3.3). In addition, they develop a homogenous morphology, strongly reminiscent of pyramidal neurons after several days in culture.

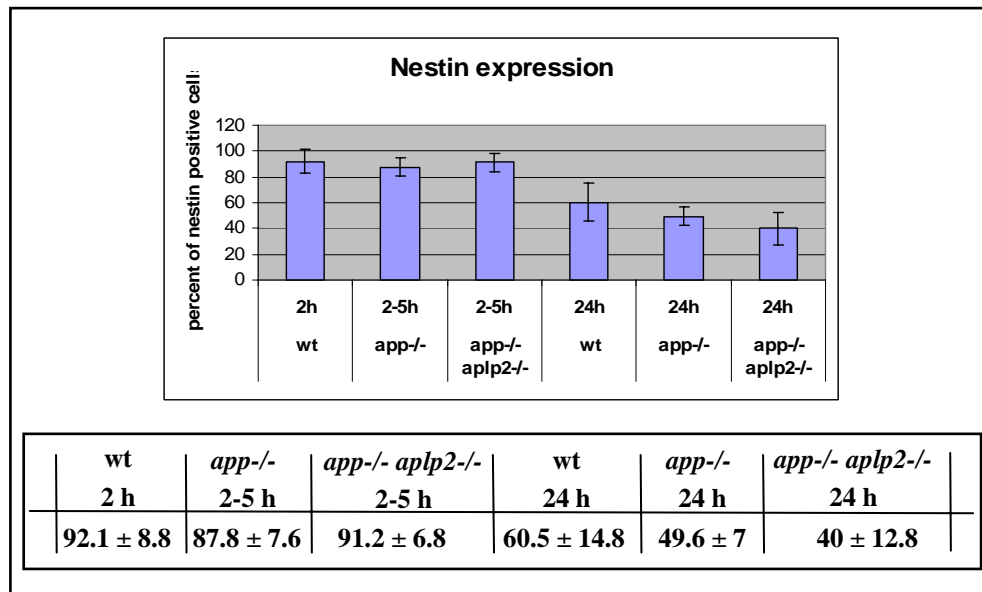


Figure 9: Quantification of the radial glial cell marker nestin

Neural progenitors derived from wild-type, *app*^{-/-} and *app*^{-/-} *aplp2*^{-/-} ES cells were fixed 2-5 and 24 hours after plating of dissociated EBs. Cells were stained with a monoclonal antibody recognizing nestin (rat 401) and with a dye, DAPI, forming fluorescent complexes with DNA. Nestin was visualized by staining with a Cy3-conjugated secondary antibody (for further details see Materials and Methods). Cells positive for nestin were counted and the percentage of positive cells was calculated in relation to the total number of cells (DAPI-positive nuclei). The results are expressed as % ± S.D.

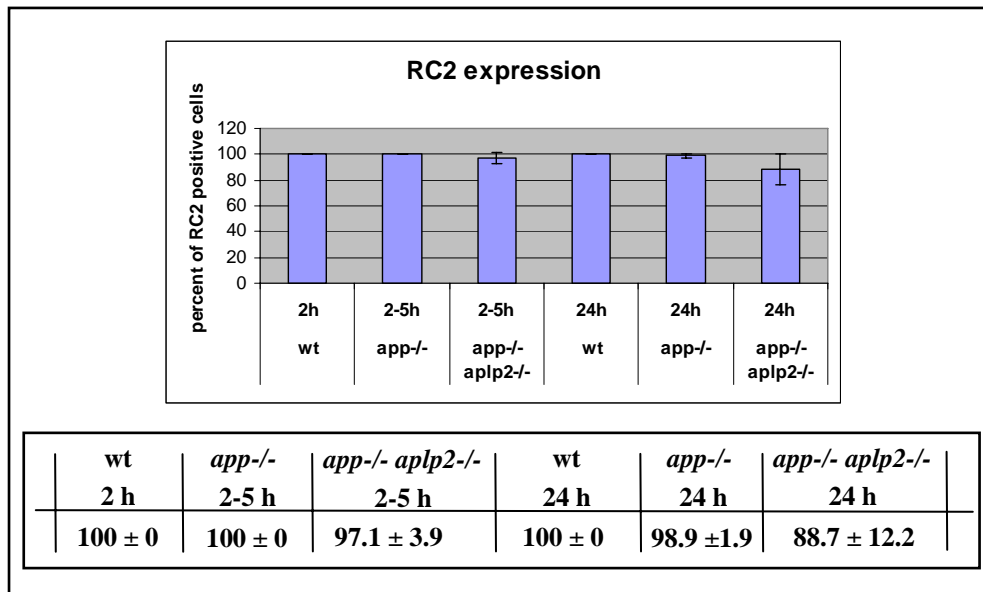


Figure 10: Quantification of the radial glial cell marker RC2

Neural progenitors derived from wild-type, *app*^{-/-} and *app*^{-/-} *apl**p*^{2-/-} ES cells were fixed 2-5 and 24 hours after plating of dissociated EBs. Cells were stained with a monoclonal antibody recognizing RC2 and with a dye, DAPI, forming fluorescent complexes with DNA. RC2 was visualized by staining with a Cy3-conjugated secondary antibody (for further details see Materials and Methods). Cells positive for RC2 were counted and the percentage of positive cells was calculated in relation to the total number of cells (DAPI-positive nuclei). The results are expressed as % ± S.D.

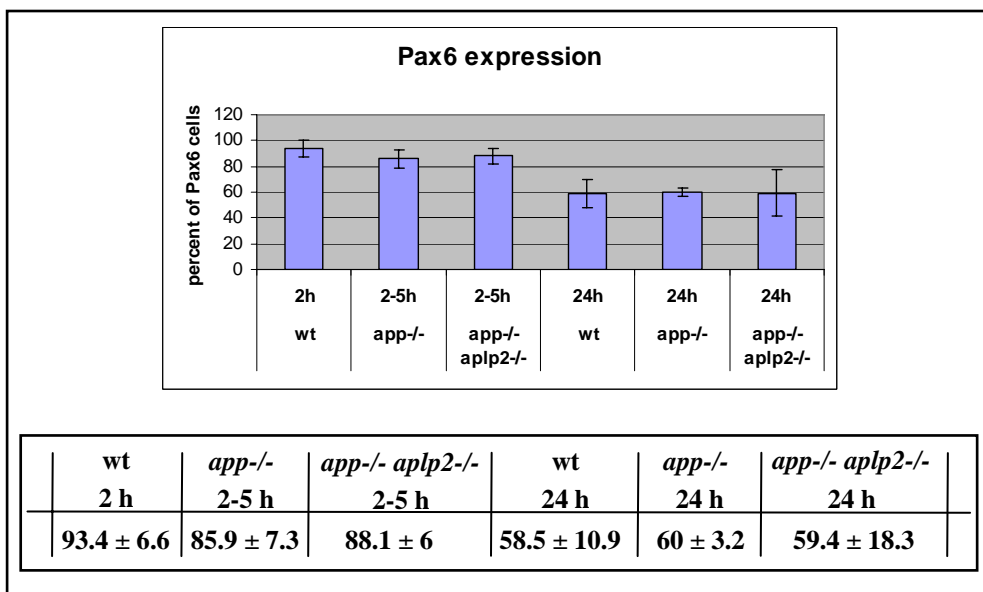


Figure 11: Quantification of Pax6 expression in radial glial cells

Neural progenitors derived from wild-type, *app*^{-/-} and *app*^{-/-} *apl**p*^{2-/-} ES cells were fixed 2-5 and 24 hours after plating of dissociated EBs. Cells were stained with a monoclonal antibody recognizing Pax6 and with a dye, DAPI, forming fluorescent complexes with DNA. Pax6 was visualized by staining with a Cy3-conjugated secondary antibody (for further details see Materials and Methods). Cells positive for Pax6 were counted and the percentage of positive cells was calculated in relation to the total number of cells (DAPI-positive nuclei). The results are expressed as % ± S.D.

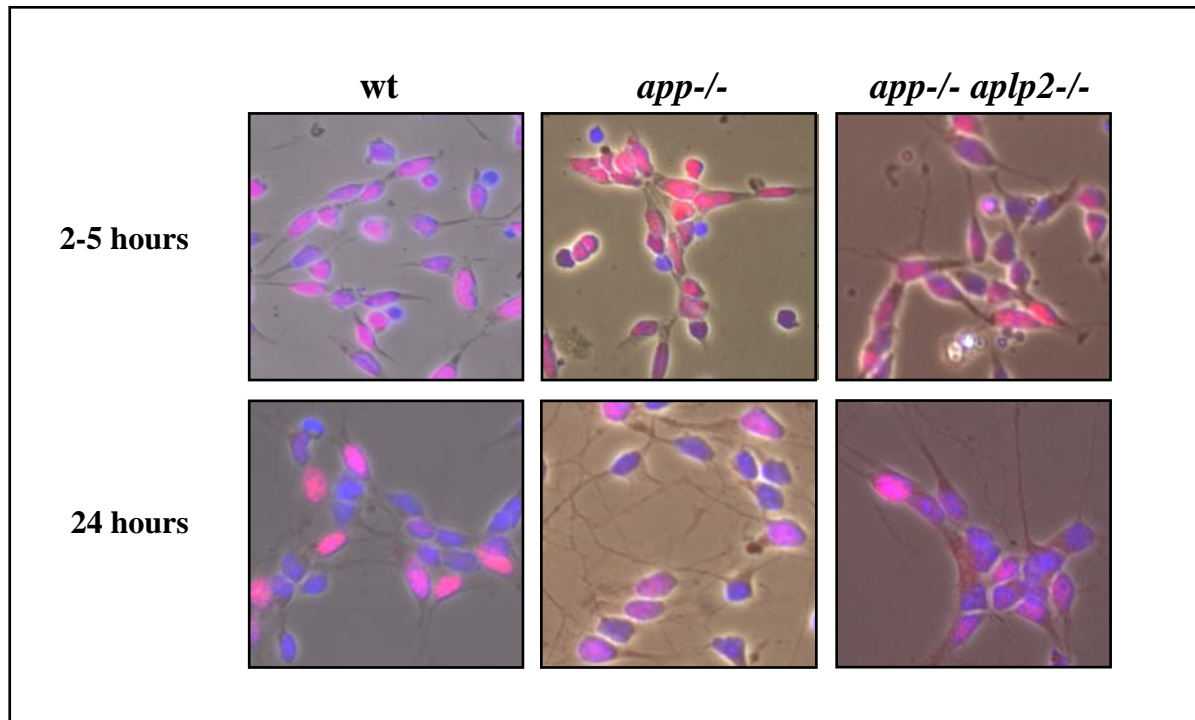


Figure 12: Pax6 immunoreactivity of radial glial cells derived from wild-type, *app*^{-/-} and *app*^{-/-} *aplp2*^{-/-} ES cells

Radial glial cells derived from wild-type, *app*^{-/-} and *app*^{-/-} *aplp2*^{-/-} ES cells were fixed after 2-5 and 24 hours and stained with a monoclonal antibody recognizing Pax6 and with a dye, DAPI, forming fluorescent complexes with DNA. Pax6 was visualized by a Cy3-conjugated secondary antibody (for further details see Materials and Methods). Pictures show the staining pattern of Pax6 as overlay of phase contrast and fluorescence images of the nuclear marker Pax6 and DAPI. In blue: DAPI, in purple: Pax6 and DAPI.

3.3 Expression of synaptic proteins in neurons lacking *app* or *app* and *aplp2*

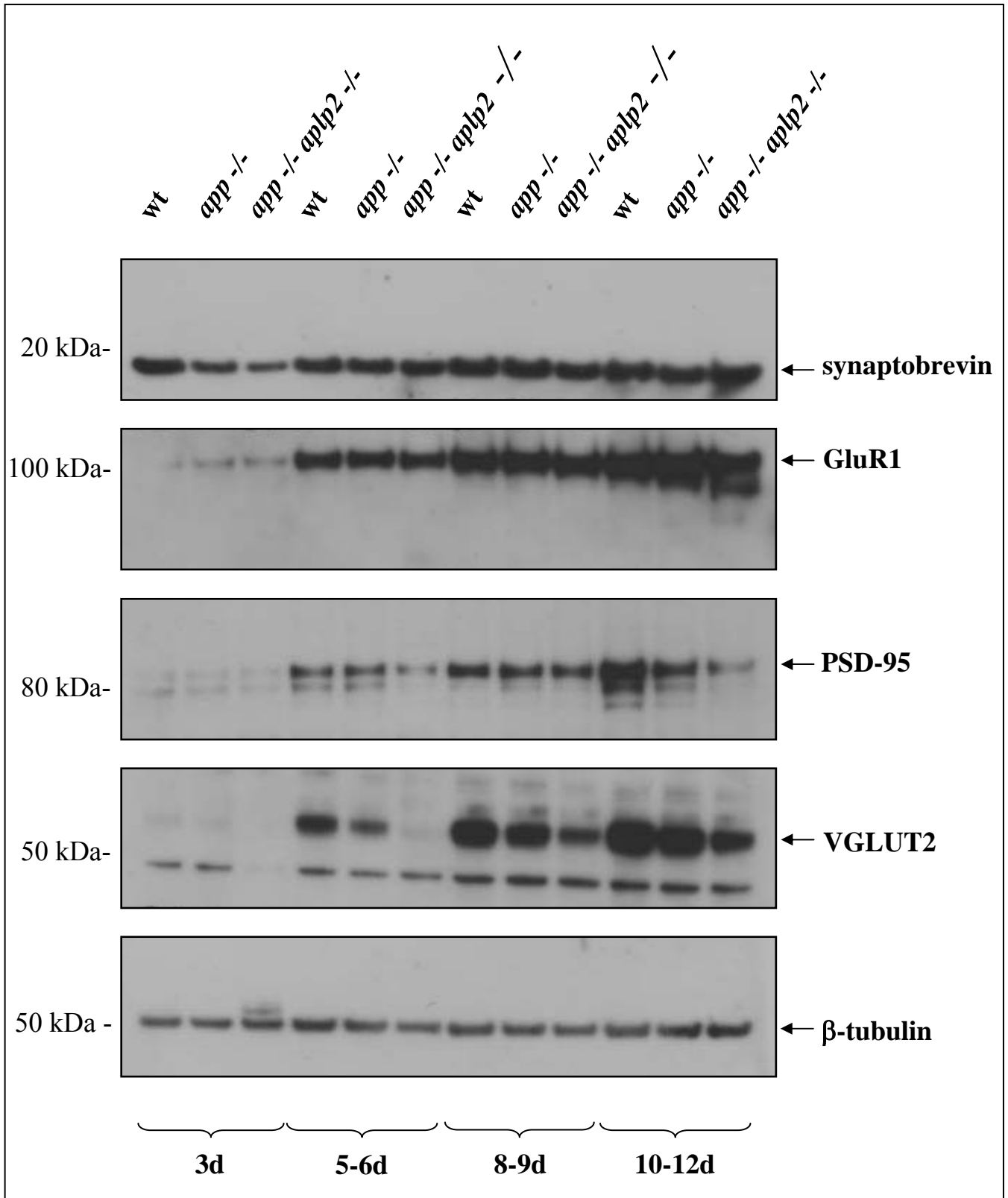
Several studies suggest a contribution of APP and its homologues in synapse formation and function (see Introduction). Because our ES cell-derived system allows us to work with neurons that develop in synchrony, we decided to investigate a possible role of APP and APLP2 during synapse formation by analyzing the expression of synaptic proteins in neurons derived from ES cells lacking *app* or *app* and *aplp2*. In protein extracts from wild-type, *app*^{-/-} and *app*^{-/-} *aplp2*^{-/-} neurons lysed after 3, 5, 6, 8, 9, 10 and 12 DIV the expression of well characterized synaptic markers including the presynaptic markers synaptobrevin and vesicular glutamate transporter 2 (VGLUT2) and postsynaptic proteins such as postsynaptic density-95 (PSD-95) and glutamate receptor subunit 1 (GluR1) was analyzed by Western

Blot. Protein amounts were adjusted such that the expression of the neuron specific markers β -tubulin or tau were similar. Comparable levels of synaptobrevin and GluR1 (Fig. 13) were found, while the expression of PSD-95 was slightly reduced in lysates from *app*^{-/-} and *app*^{-/-} *aplp2*^{-/-} neurons. By contrast, a remarkable reduction in the expression of VGLUT2 could be observed in neurons lacking *app* as well as *app* and *aplp2*. Reduction of VGLUT2 expression seemed to be more significant in *app*^{-/-} *aplp2*^{-/-} than in *app*^{-/-} neurons (Fig. 13) suggesting a gene dosage dependency. However, decrease of VGLUT2 in *app*^{-/-} neurons was not always consistent, possibly due to the presence of APLP2. In view of this, we subsequently focused on the comparison of wild-type versus *app*^{-/-} *aplp2*^{-/-} neurons.

According to previous electrophysiological recordings (Bibel et al., 2004) we considered neurons after 12 DIV as having mature synapses and therefore, all further studies were performed with neurons that had been in culture for at least 12 days (12 DIV).

Figure 13 (next page): Expression of synaptic proteins in wild-type, *app*^{-/-} and *app*^{-/-} *aplp2*^{-/-} neurons

Western Blots were performed with protein extracts taken from wild-type, *app*^{-/-} and *app*^{-/-} *aplp2*^{-/-} neurons after 3, 5, 6, 8, 9, 10 and 12 DIV. Volumes of protein extracts loaded on 10% Tris-Bis gels were normalized to volumes representing equal amounts of β -tubulin protein. After protein transfer the membranes were either probed with a monoclonal antibody recognizing synaptobrevin/VAMP2 (18 kDa), a polyclonal antibody recognizing VGLUT2 (~65 kDa), a monoclonal antibody recognizing PSD-95 (95 kDa) or a polyclonal antibody recognizing the glutamate receptor subunit 1, GluR1 (100 kDa). For normalization a monoclonal antibody recognizing the neuron specific β -tubulin was used (50 kDa) (for antibody dilutions and further details see Materials and Methods). VGLUT2 and PSD-95 appear differentially expressed whereas synaptobrevin and GluR1 do not.



Western Blots with extracts from wild-type and *app*^{-/-} *aplp2*^{-/-} neurons after 12 DIV normalized for similar levels of tau showed a strong decrease in VGLUT2 expression while synaptophysin did not seem to be changed (Fig. 14). The reduction of VGLUT2 protein expression was confirmed in 7 independent differentiations of ES cells lacking APP and APLP2 compared to 6 independent differentiations of wild-type neurons.

The expression of VGLUT1, another vesicular glutamate transporter, was also tested in wild-type and *app*^{-/-} *aplp2*^{-/-} neurons. It showed a very similar expression pattern as VGLUT2 that led us to doubt the specificity of the VGLUT1 antibody (data not shown). As both transporters are strongly related in their amino acid sequence (82%) the antibodies might cross-react.

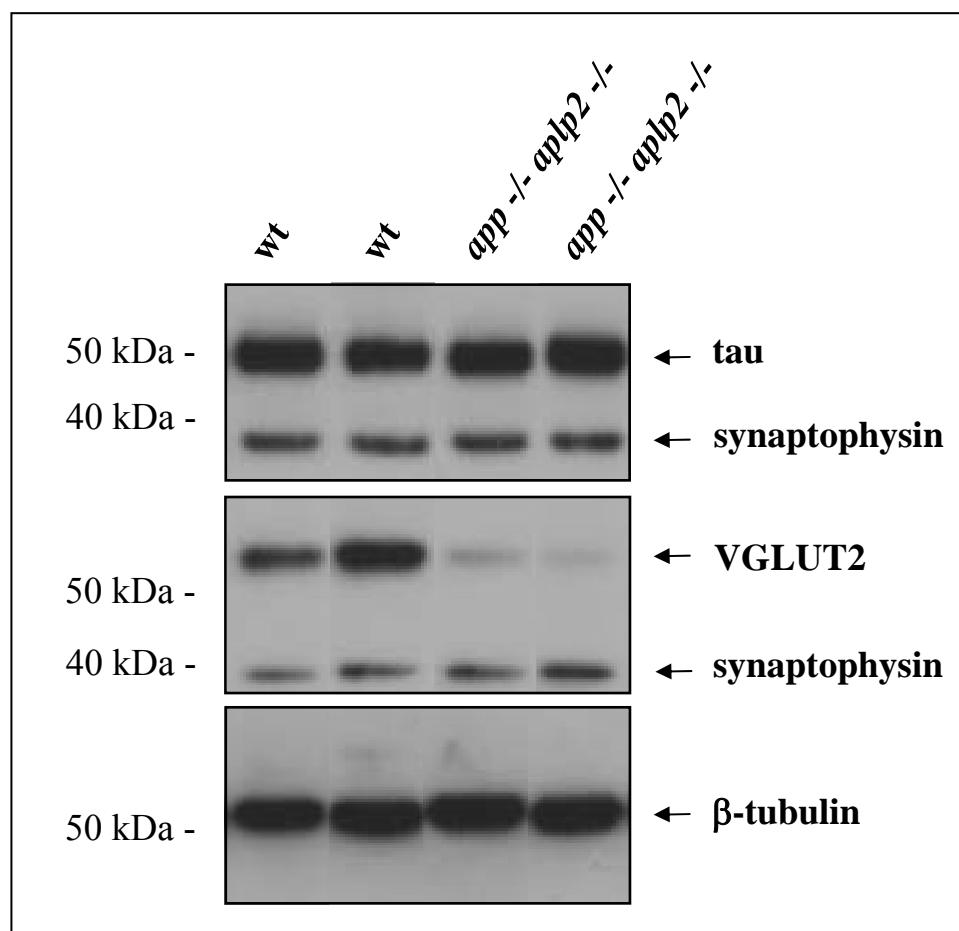


Figure 14: Expression of synaptic proteins in wild-type and *app*^{-/-} *aplp2*^{-/-} neurons after 12 DIV

Western Blots were performed with protein extracts from wild-type and *app*^{-/-} *aplp2*^{-/-} neurons after 12 DIV. Volumes of protein extracts loaded on 10% Tris-Bis gels were normalized to volumes representing equal amounts of tau protein. After protein transfer the membranes were either probed with a polyclonal antibody recognizing VGLUT2 (~65 kDa), a monoclonal antibody recognizing synaptophysin (38 kDa) or a monoclonal antibody recognizing the neuron specific β -tubulin (50 kDa). For normalization a monoclonal antibody recognizing tau (tau-1; ~50 kDa) was used (for antibody dilutions and further details see Materials and Methods). Note the strong reduction in VGLUT2 expression in *app*^{-/-} *aplp2*^{-/-} neurons.

3.4 *Vglut2* transcription in wild-type and *app*^{-/-} *aplp2*^{-/-} neurons

The observed reduction of VGLUT2 protein could be either the result of changes in *vglut2* transcription or translation. To investigate if the transcription of *vglut2* is altered in the absence of *app* and *aplp2*, we performed quantitative RT-PCR and compared the levels of *vglut2* transcript in wild-type and double knock-out neurons. We included synaptophysin as a control, as we did not observe any change at the protein level. RNA was isolated from wild-type and *app*^{-/-} *aplp2*^{-/-} neurons after 12 DIV and quantitative RT-PCR was carried out using the TaqMan system as described in Materials and Methods. RNA levels of *vglut2* and *synaptophysin* genes were normalized to *tau*. Tau RNA levels were normalized to 18S ribosomal RNA (18S).

By comparing 5 independent wild-type with 10 independent *app*^{-/-} *aplp2*^{-/-} differentiations we detected a strong decrease in the transcription of the *vglut2* gene in neurons lacking *app* and *aplp2* while *synaptophysin* transcription was not significantly changed (Fig. 15 and Fig. 16). Variations in tau as well as in synaptophysin RNA levels could be observed, presumably due to fluctuations of culture quality. However, these variations had no influence on the reduction of VGLUT2 RNA levels. The results of the quantitative RT-PCR were supported by semi-quantitative RT-PCR data, where a strong reduction in the *vglut2* transcription could be observed as well (Fig. 17).

As we were not able to clearly identify VGLUT1 at the protein level because of a possible cross-reactivity of the antibody with VGLUT2, we examined the presence of VGLUT1 at the RNA level. Therefore, we performed quantitative RT-PCR for *vglut1* transcripts. As the levels detected in wild-type and double knock-out neurons were only slightly above background levels (data not shown), we conclude that the *vglut1* gene is expressed in neurons derived from both ES cell lines only at very low copy numbers. This result further suggests that the VGLUT1 antibody very likely recognizes VGLUT2 in Western blot experiments.

Thus, we conclude that the deletion of *app* and *aplp2* affects transcription of *vglut2* and that the reduction of VGLUT protein is accounted for a reduction in VGLUT2, as opposed to VGLUT1, which seems to be expressed at very low levels.

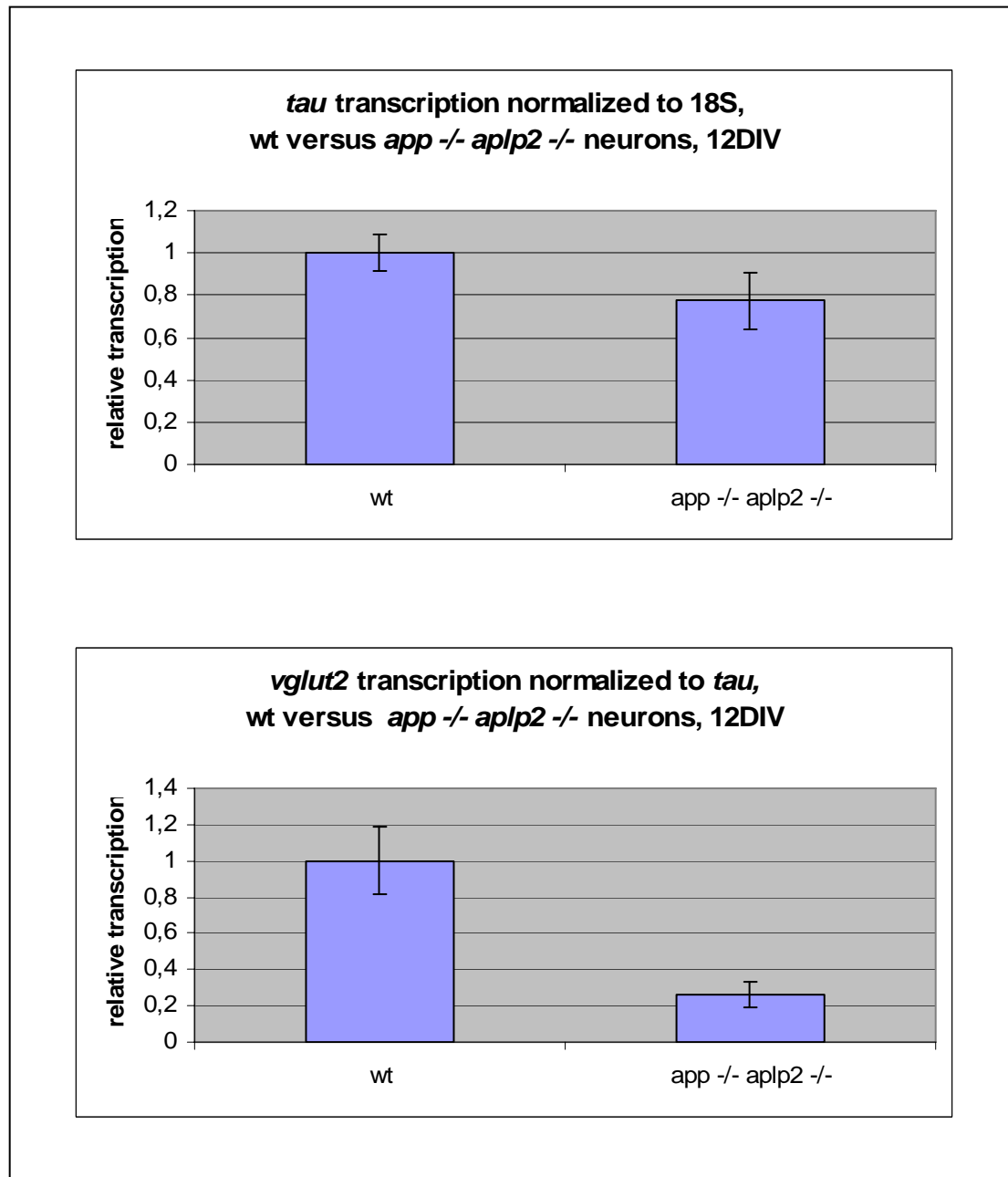


Figure 15: Vglut2 transcription in wild-type and *app*^{-/-} *aplp2*^{-/-} neurons assessed by quantitative RT-PCR

Transcription of *tau* and *vglut2* in wild-type and *app*^{-/-} *aplp2*^{-/-} neurons after 12 DIV was performed using quantitative RT-PCR. RNA was isolated and cDNA synthesis performed as described in Materials and Methods. Transcription of *vglut2* and *tau* was assessed using inventoried assays from Applied Biosystems and primers and probe designed with primer express software from ABI, respectively. *Vglut2* transcription was normalized to *tau* transcription while *tau* itself was normalized to 18S. Results from 3 independent PCRs performed with one cDNA are shown as mean of 4 independent differentiations of either genotype \pm S.D. Note the strong decrease of *vglut2* transcription in *app*^{-/-} *aplp2*^{-/-} neurons normalized to *tau*.

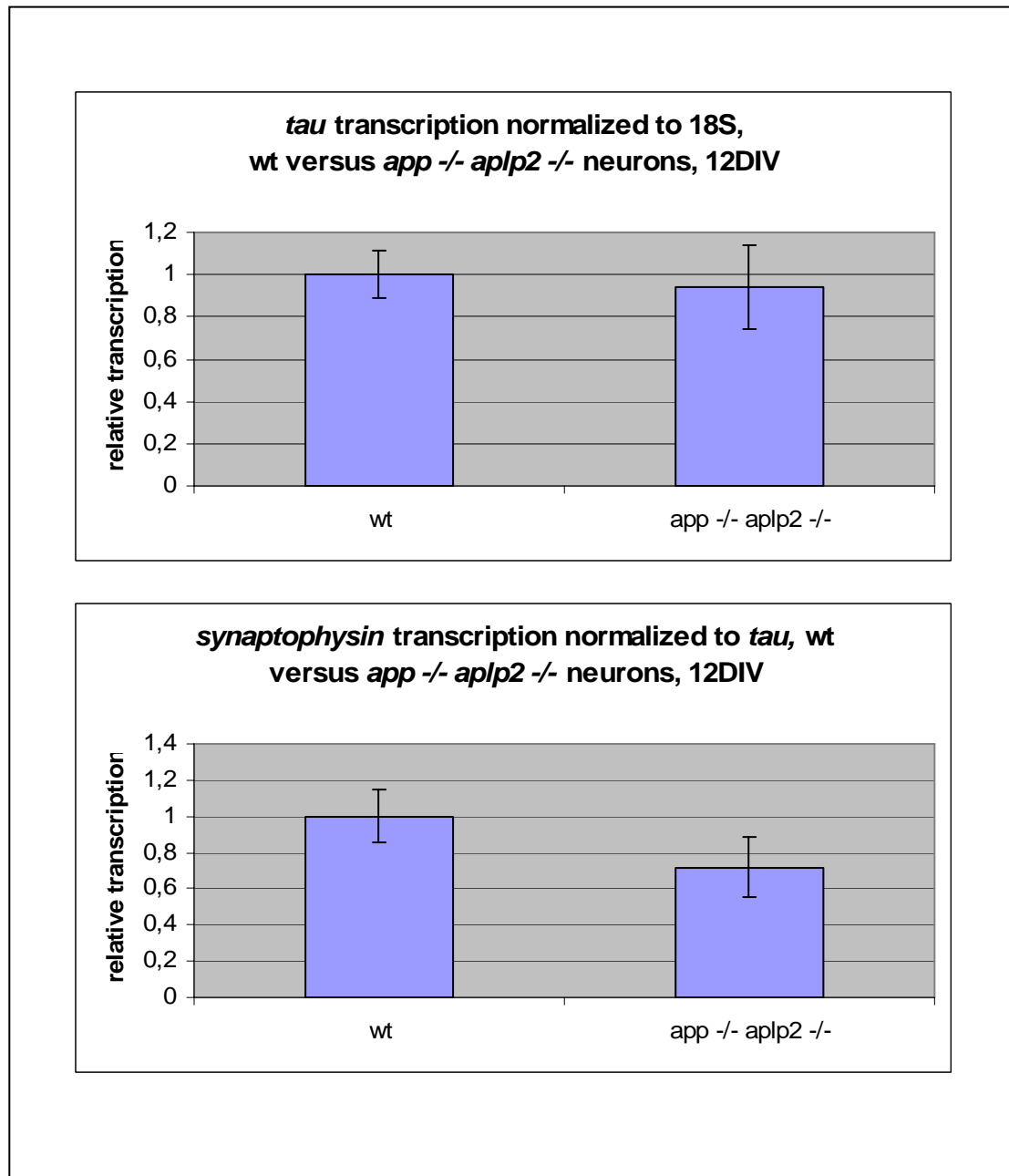


Figure 16: Synaptophysin transcription in wild-type and *app*^{-/-} *aplp2*^{-/-} neurons assessed by quantitative RT-PCR

Transcription of *tau* and *synaptophysin* in wild-type and *app*^{-/-} *aplp2*^{-/-} neurons after 12 DIV was performed using quantitative RT-PCR. RNA was isolated and cDNA synthesis performed as described in Materials and Methods. Transcription of *synaptophysin* and *tau* was assessed using inventoried assays from Applied Biosystems and primers and probe designed with primer express software from ABI, respectively. *Synaptophysin* transcription was normalized to *tau* transcription while *tau* itself was normalized to 18S. Results from 3 independent PCRs performed with one cDNA are shown as mean of 4 independent differentiations of either genotype \pm S.D. Synaptophysin RNA levels were not significantly different between wild-type and *app*^{-/-} *aplp2*^{-/-} neurons normalized to *tau*.

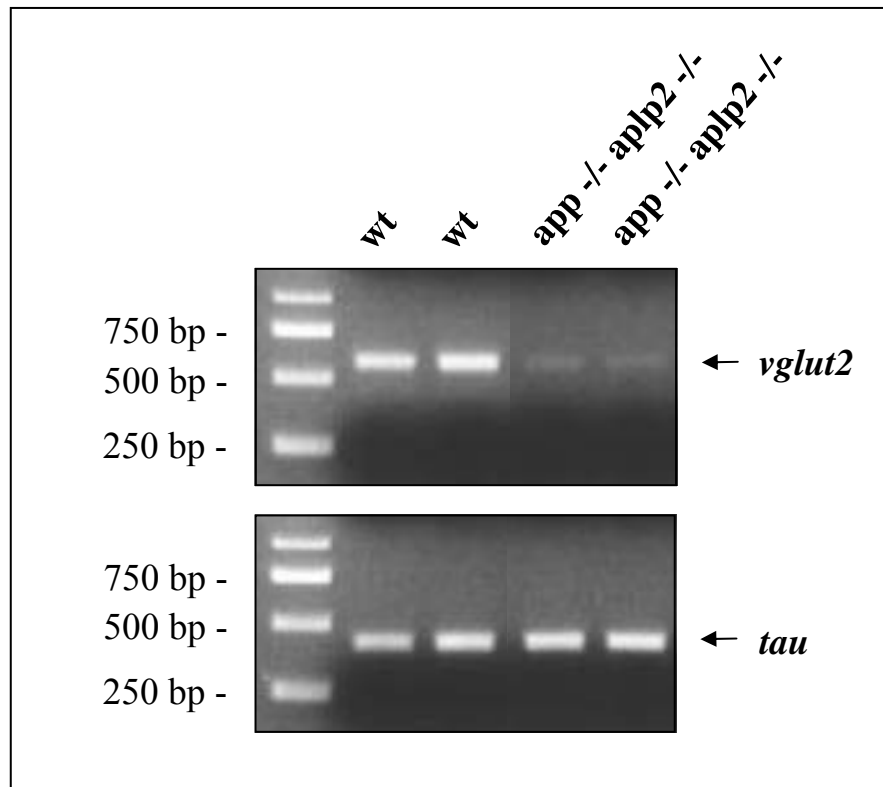


Figure 17: *Vglut2* transcription in wild-type and *app*^{-/-} *aplp2*^{-/-} neurons assessed by semi-quantitative RT-PCR

Transcription of *vglut2* in wild-type and *app*^{-/-} *aplp2*^{-/-} neurons after 12 DIV was performed using semi-quantitative RT-PCR. RNA was isolated and cDNA synthesis performed as described in Materials and Methods. Primers for *tau* detection amplify a fragment of 422 bp length and primers for *vglut2* detection amplify a fragment of 594 bp length. Note the strong decrease in VGLUT2 RNA levels in *app*^{-/-} *aplp2*^{-/-} neurons.

3.5 Release of glutamate in wild-type and *app*^{-/-} *aplp2*^{-/-} neurons

VGLUT1 and VGLUT2 are the main vesicular glutamate transporters in glutamatergic neurons. As our results indicate, only VGLUT2 is expressed at appropriate levels in our ES cell system and is strongly reduced after 12 DIV in *app*^{-/-} *aplp2*^{-/-} neurons. Therefore it was of interest to test if the release of glutamate is affected in these cells. To explore this possibility, we investigated the glutamate release of wild-type and double knock-out neurons.

Neurons after 14 DIV were incubated with ³[H]-labeled glutamate (³[H]-glu) and the subsequent release of ³[H]-glu after stimulation was monitored. The neurons were stimulated either with KCl (50 mM) or

glutamate (glu, 100 μ M; for further details see Materials and Methods). KCl leads to a general depolarization of neurons by increasing the intracellular $[Ca^{2+}]_i$ concentrations, while glutamate causes a more local depolarization through the activation of glutamate receptors. Stimulation by either means result in neurotransmitter release. Neurons were stimulated twice (after 25 and 45 min) and medium fractions were collected before and after stimulation, to compare counts of $^3[H]$ -glu between the two genotypes (Fig. 18).

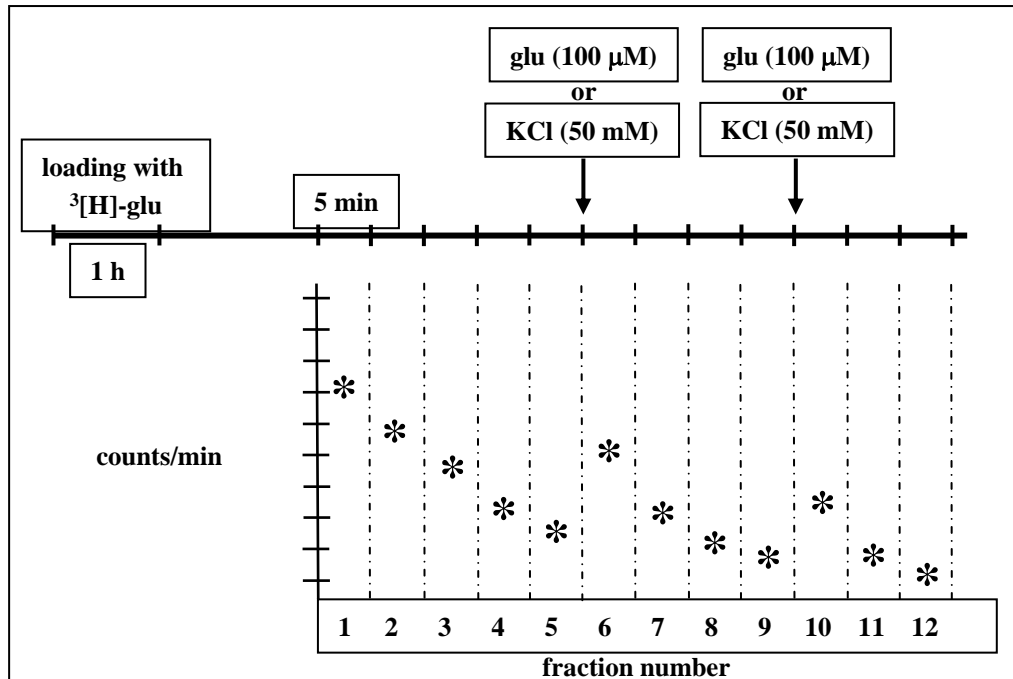


Figure 18: Experimental paradigm for glutamate release assay

Diagram of the experimental set-up for measuring glutamate release. Neurons (14 DIV) were incubated for 1 hour with $^3[H]$ -glu at 37°C. Cultures were washed several times with HANKS buffer before medium fractions were collected every 5 min and replaced by fresh medium. After 25 and 45 min KCl or glutamate was added. The fractions were analyzed with a scintillation counter. Stars depict the expected progression of $^3[H]$ -labeled glutamate release.

Without application of depolarizing concentrations of KCl or glutamate, a slow decline of $^3[H]$ -glu in the collected fractions was observed related to glutamate release after spontaneous neuronal activity (Fig. 19). In contrast, after the neurons had been stimulated for the first time, significant amounts of labeled glutamate were released, while the amount released after the second stimulus was much lower as the system depletes of $^3[H]$ -glu (Fig. 19). The comparison of the amounts of labeled glutamate released by neurons from both genotypes reveals a clear decrease in the release ability of neurons lacking *app* and *aplp2*, both after KCl and glutamate stimulation (Fig. 20).

Thus, the reduction in VGLUT2 expression results in a functional readout and we conclude that the decrease in glutamate release is a consequence of the combined absence of APP and APLP2.

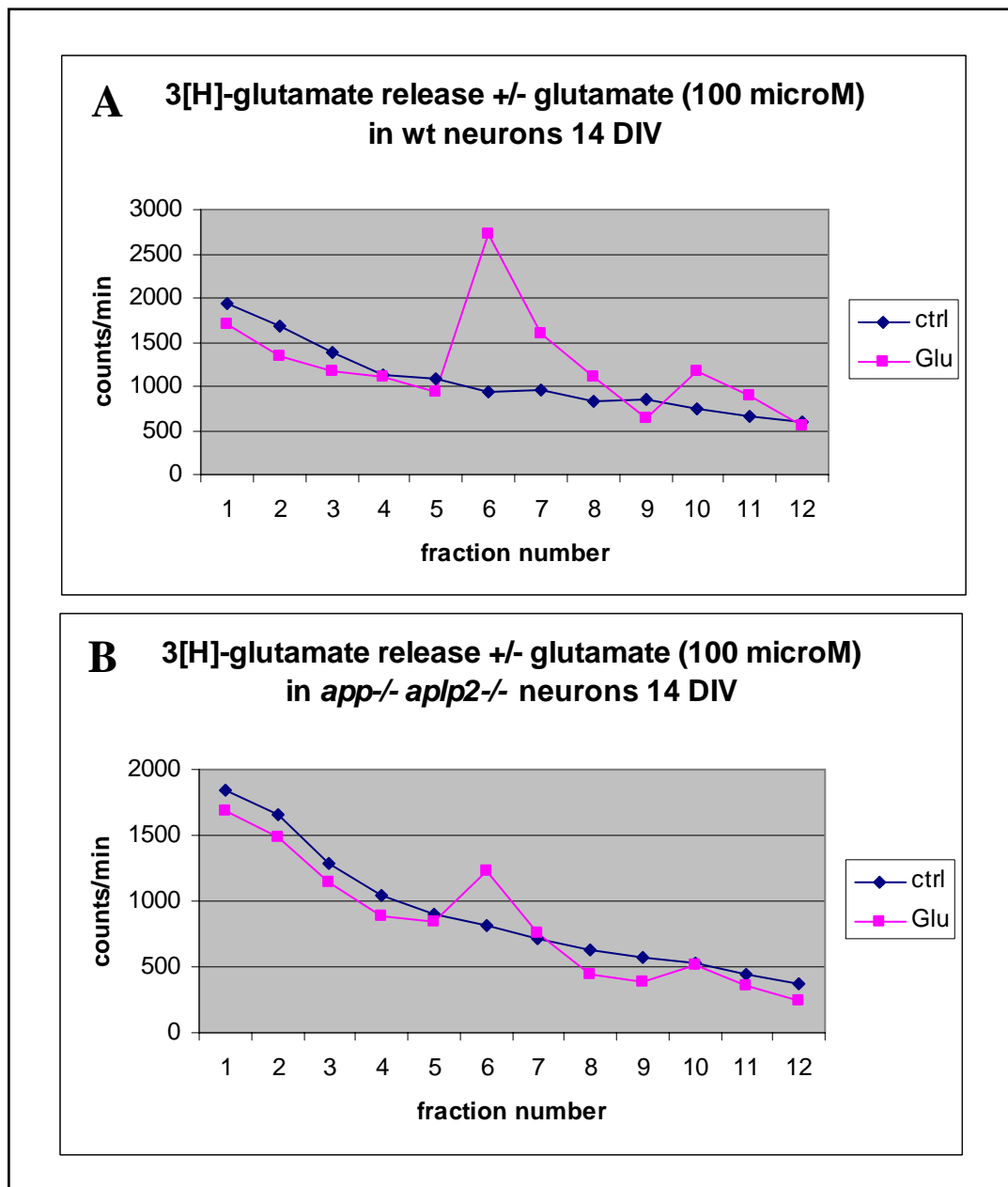


Figure 19: Glutamate release of wild-type and *app*^{-/-} *apl2*^{-/-} neurons

Example of a representative glutamate release curve. A) Wild-type neurons (wt) loaded with ³[H]-glu, were stimulated (pink curve) or not (blue curve) with glutamate (100 μM). The stimulation pulse was given after fraction 5 and 9 and resulted in an increase in glutamate in fraction 6 and 10. Without stimulation ³[H]-glu was released slowly over time. B) Neurons lacking *app* and *apl2* were treated as the wild-type neurons in A) but showed a reduced glutamate release peak in fraction 6 and 10 after stimulation compared to wild-type neurons.

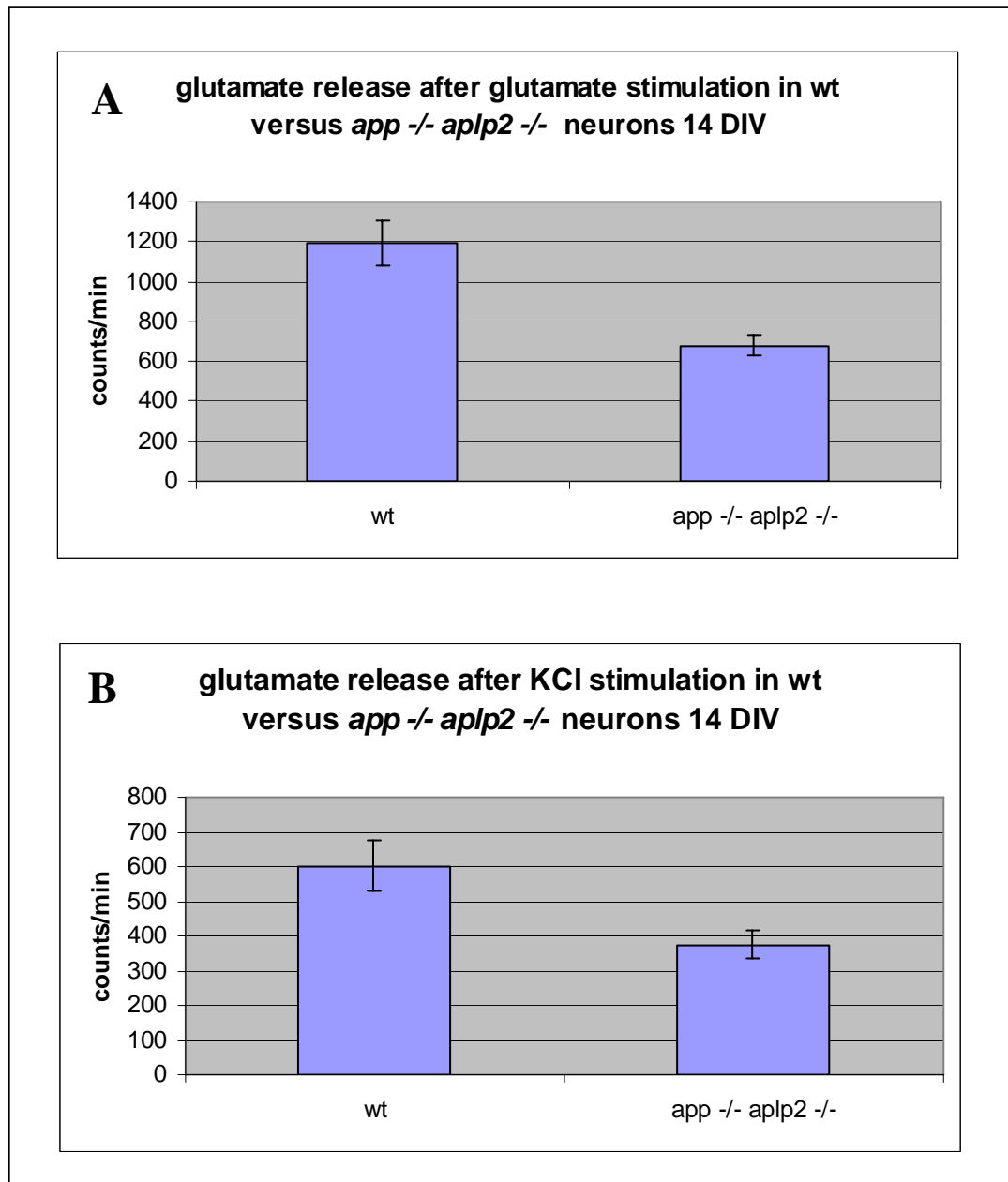


Figure 20: Quantification of glutamate release

Counts of released ³[H]-labeled glutamate after the first stimulation were compared between wild-type (wt) and *app*^{-/-} *aplp2*^{-/-} neurons (for analysis paradigm see Materials and Methods). Experiments are shown as mean ± S.E. of two to three independent differentiations. Glutamate release is strongly reduced in *app*^{-/-} *aplp2*^{-/-} neurons either after KCl or glutamate stimulation.

3.6 *Vglut2* transcription after γ -secretase inhibitor treatment

The observed reduction in *vglut2* transcription suggests a contribution of the two APP family members in transcriptional regulation. Recently, a small intracellular fragment of APP and APLP2 (AICD and ALICD2; Passer et al., 2000; Scheinfeld et al., 2002), generated by γ -secretase cleavage, has been shown to function as a transcriptional regulator (Cao et al., 2001).

Our finding led us to the hypothesis that *vglut2* might be a target gene for the AICD modulated transcriptional process.

To get insight into the mechanism involved, we attempted to block the generation of the AICD fragment by treating wild-type neurons with a γ -secretase inhibitor. γ -secretase is known to cleave a broad range of transmembrane proteins including Notch that is involved in cell-fate determination. As we can not exclude an impairment of the Notch pathway by the inhibitor we used, we treated the cells after they had been in culture for at least 6 days and already display neuronal characteristics. Wild-type neurons were treated with LY411575 (50 nM), a highly potent γ -secretase inhibitor with an IC_{50} of < 1 nM in HEK cells (Schmidt 2003; Larbig et al., 2004). The inhibitor was applied either only after 6 DIV, 11 DIV or 6 and 11 DIV and RNA was extracted after 12 DIV. Levels of *vglut2* and *synaptophysin* transcripts were evaluated by quantitative RT-PCR and normalized to 18S. 6 independent wild-type cultures were treated with γ -secretase inhibitor and in 5 of them we could see a decrease in *vglut2* transcription, while the transcription of *synaptophysin* was not affected (Fig. 21). Treatment for 6 days *in vitro* led to a stronger inhibition than only treating after 11 days. However, degree of downregulation was found to be varying for reasons that are not entirely clear.

Nonetheless, we feel that these findings support the possibility that *vglut2* may be regulated at the transcriptional level by a proteolytical product of APP and/or APLP2.

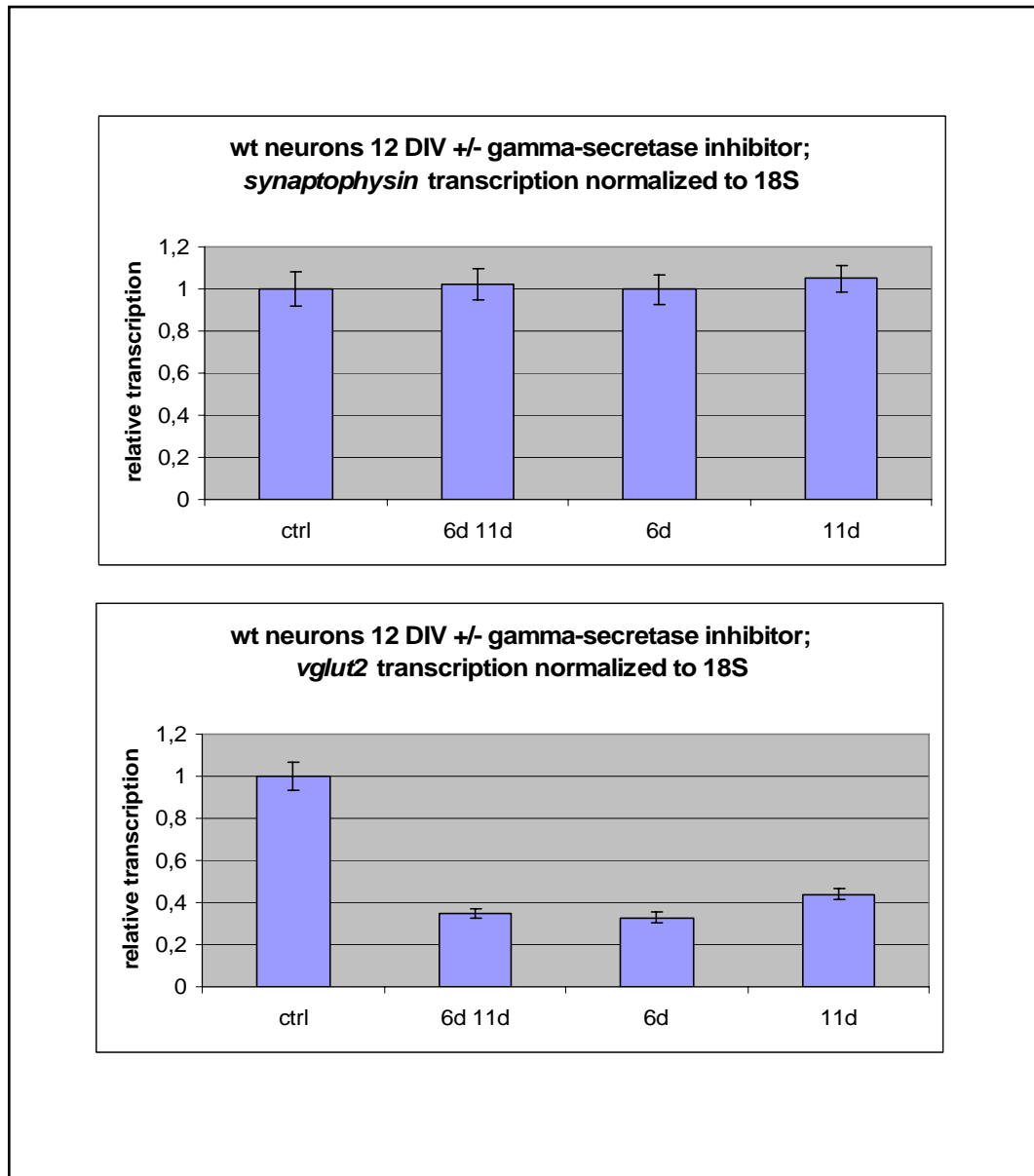


Figure 21: Treatment of wild-type neurons with γ -secretase inhibitor

Wild-type (wt) neurons were treated with 50 nM γ -secretase inhibitor after 6, 11, or 6 and 11 days *in vitro*. RNA was extracted after 12 DIV and cDNA was synthesized as described in Materials and Methods. *Vglut2* and *synaptophysin* transcription were evaluated by quantitative RT-PCR using inventoried detection assays from Applied Biosystems. Figures depict the transcription profile of one treated culture. Bars show mean of 3 independent PCRs performed from one cDNA \pm S.D. Note the reduction of *vglut2* transcription normalized to 18S after treatment with γ -secretase inhibitor while *synaptophysin* transcription was not changed.

3.7 Levels of VGLUT2 protein and RNA in neurons expressing human APP in addition to endogenous mouse APP

As our findings suggest an involvement of APP and APLP2 in *vglut2* transcription, we were interested to see if the presence of additional APP at early time points of neuronal development would give rise to the opposite effect, that is an increase in *vglut2* transcripts and protein.

To test this possibility, we made use of an ES cell line, termed E3#8, expressing human APP (hAPP) in addition to endogenous mouse APP. The E3#8 ES cell line was generated by targeting the cDNA for hAPP into the locus encoding the microtubule-binding protein tau. Using this strategy, the expression of hAPP is driven by the endogenous *tau* promoter. In addition to hAPP the second tau allele was targeted with the cDNA for enhanced green fluorescent protein (EGFP) (*tau^{tau:egfp/tau:hAPP}*) and thus neurons derived from this cell line express hAPP and EGFP driven by the endogenous *tau* promoter. As wild-type line we used ES cells expressing only EGFP driven by the endogenous *tau* promoter (*tau^{tau:egfp/tau}*; named E3) which enabled us to normalize all data to similar levels of EGFP. The E3#8 cell line had already been successfully used for human A β ₄₀ detection by a highly sensitive ELISA (data not shown). The production of A β ₄₀ confirms the presence of human APP protein in the neurons and its cleavage by endogenous β - and γ -secretase.

Following their differentiation in neurons, we wanted to study if in the E3#8 cell line additional APP protein would increase the transcription of *vglut2* and result in higher levels of VGLUT2 protein. As APP expression increases strongly during the course of neuronal differentiation we decided to examine neurons at early time points. At day 4, the *tau* promoter has been shown to be already active and human APP is transcribed while endogenous mouse APP has not yet reached a stable level. Therefore, additional protein might exert an effect on *vglut2* transcription at this time point that can be monitored. In addition, according to our Western data VGLUT2 protein can be first detected after 5-6 DIV (Chapter 3.3). Accordingly, we studied the levels of *vglut2* transcript and VGLUT2 protein from neurons that had been in culture for 5, 6 and 8 days. We performed quantitative RT-PCR and observed in 4 out of 5 independent differentiations a clear increase in *vglut2* transcription after 6 DIV in neurons derived from E3#8 ES cells compared to E3 derived neurons (Fig. 22). Western Blot analysis did show increased VGLUT2 protein levels in some, but not all neurons derived from E3#8 compared to neurons

derived from E3 (Fig. 23). Because of the time delay between gene transcription and protein synthesis we might have missed the optimal time window to detect a possible increase in protein level in all neurons examined.

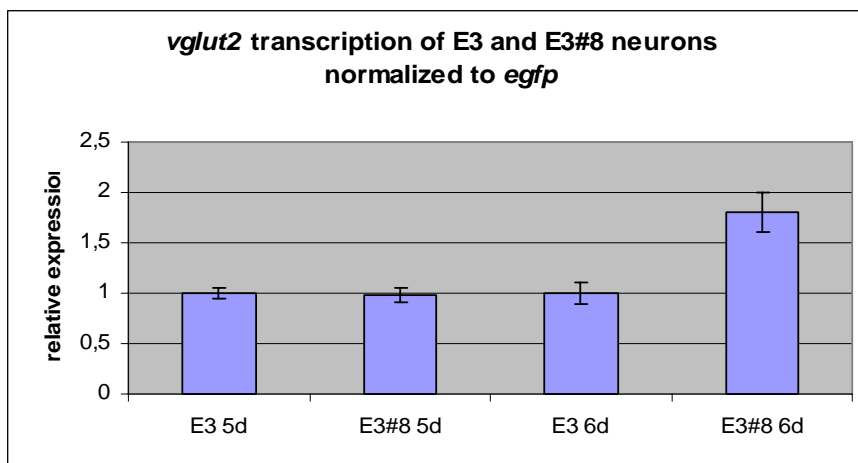


Figure 22: *Vglut2* transcription in neurons derived from E3 and E3#8 ES cells assessed by quantitative RT-PCR

Transcription of *vglut2* in neurons derived from E3 and E3#8 was evaluated using quantitative RT-PCR. RNA was extracted from neurons after 5, 6 and 8 DIV and cDNA was synthesized as described in Materials and Methods. *Vglut2* and *egfp* transcription was assessed using inventoried assays from Applied Biosystems and primers and probe designed with primer express software from ABI, respectively. *Vglut2* transcription was normalized to *egfp*, while *egfp* was normalized to 18S RNA levels. Note the increase of *vglut2* transcripts after 6 DIV.

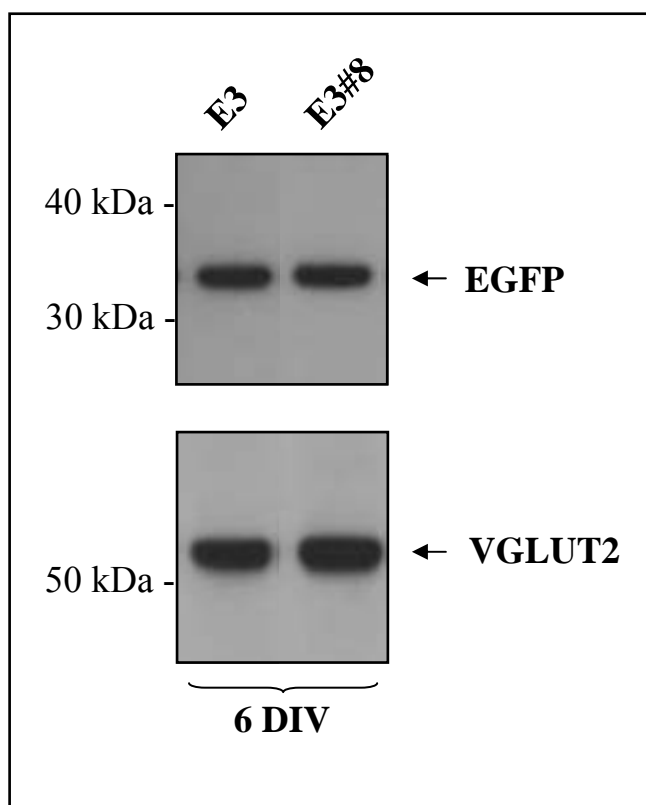


Figure 23: Detection of VGLUT2 protein levels in neurons derived from E3 and E3#8 ES cells by Western Blot analysis

Western Blot analysis was performed with protein extracts from neurons derived from E3 and E3#8, after 5, 6 and 8 DIV. Volumes of protein extracts loaded on 10% Tris-Bis gels were normalized to volumes representing equal amounts of EGFP protein. After protein transfer the membranes were either probed with a polyclonal antibody recognizing VGLUT2 (~65 kDa) or a polyclonal antibody recognizing EGFP (~35 kDa) (for antibody dilutions and further details see Materials and Methods). Note the slight increase of VGLUT2 protein after 6 DIV in these samples.

To prove that the increase in *vglut2* transcription correlates with increased levels of APP, we performed Western blot analysis with an antibody specific for human APP (6E10). In protein extracts isolated from neurons after 5, 6 and 8 DIV, increasing levels of human APP could be observed (Fig. 24). However, when we investigated the amount of total APP (human and endogenous mouse APP) with an antibody recognizing APP from both species (APP C8) we were not able to detect higher levels of total APP in neurons derived from E3#8 ES cells compared to wild-type neurons (Fig. 25).

It seems that neurons derived from E3#8 ES cells express hAPP in addition to endogenous mouse APP, but that the total amount of APP is not significantly increased compared to wild-type levels. Therefore, we are not able to unambiguously link the increased *vglut2* transcription to additionally expressed hAPP.

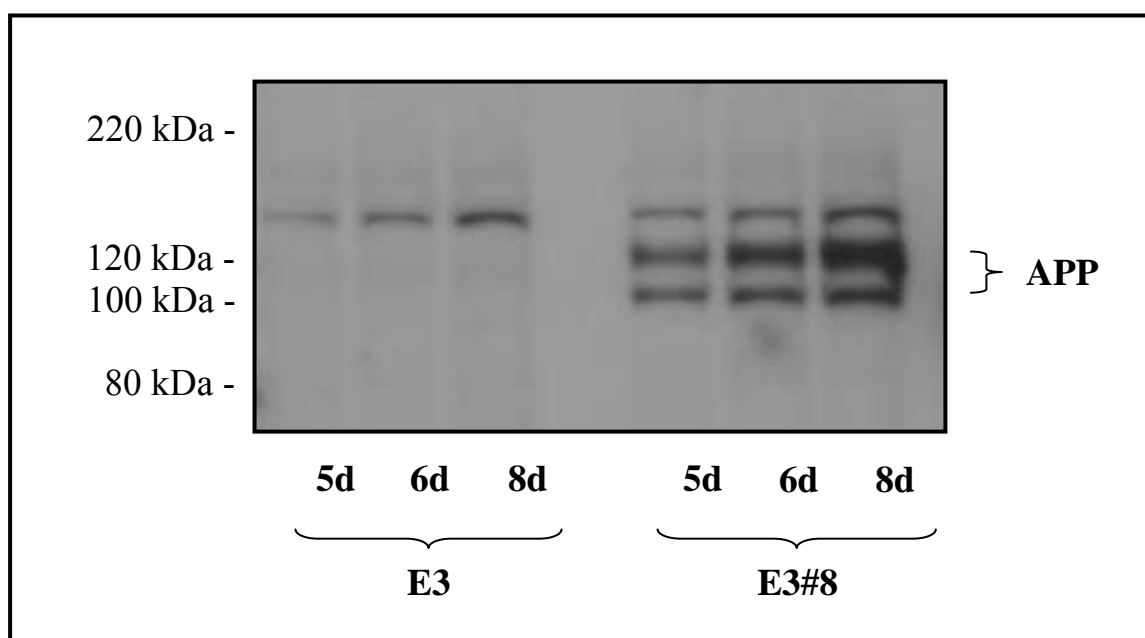


Figure 24: Detection of human APP levels in neurons derived from E3 and E3#8 ES cells by Western Blot analysis

Western Blot analysis was performed with protein extracts from E3 and E3#8 neurons after 5, 6 and 8 DIV. Equal volumes of protein extracts were loaded on a 10% Tris-Bis gel. After protein transfer the membrane was probed with a polyclonal antibody recognizing the amyloid β sequence of human APP (6E10). 10-fold more protein than usually was loaded (for antibody dilution see Materials and Methods) and the APP protein was detected between 100–120 kDa. Increasing amounts of human APP were detected during the course of differentiation in neurons from E3#8 ES cells while neurons from E3 ES cells did not show a specific band at the expected molecular weight.

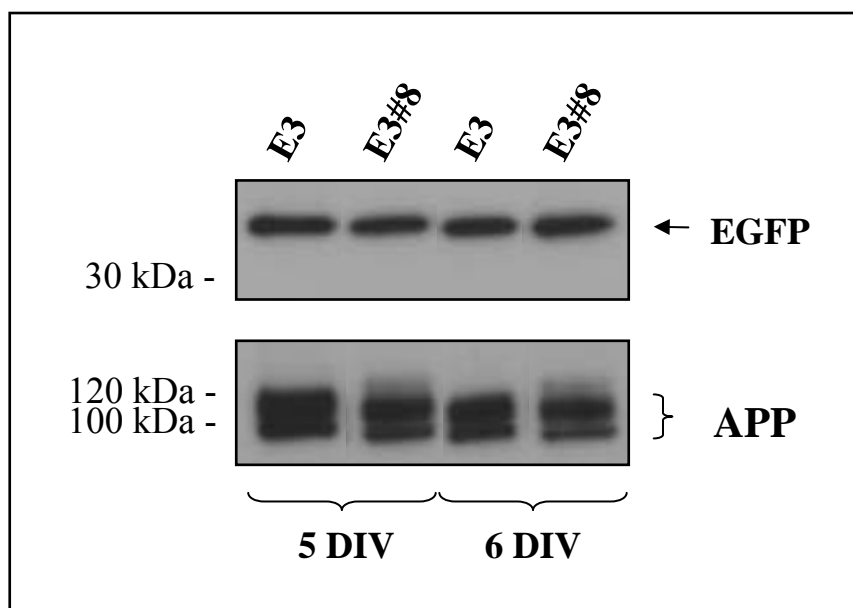


Figure 25: Detection of total APP protein levels in neurons derived from E3 and E3#8 ES cells by Western Blot analysis

Western Blots were performed with protein extracts from E3 and E3#8 neurons after 5, 6 and 8 DIV. Volumes of protein extract loaded on 10% Tris-Bis gels were normalized to volumes representing equal amounts of EGFP protein. After protein transfer the membranes were either probed with a polyclonal antibody recognizing EGFP (~35 kDa) or with a polyclonal antibody recognizing the C-terminus of human and mouse APP (APP C8) (for antibody dilutions and further details see Materials and Methods).

Note that there is no detectable increase in total amount of APP in extracts from E3#8 compared to E3.

Discussion

The main finding obtained during the course of this studies is an altered expression of synaptic components such as vesicular glutamate transporters (VGLUTs) and postsynaptic density proteins in neurons derived from ES cells lacking both *app* and *aplp2*. In addition, γ -secretase inhibitor experiments suggests that cleavage of APP and APLP2 and the release of their cytoplasmic domain is needed for appropriate transcription of the corresponding genes.

4.1 Vesicular glutamate transporters (VGLUTs)

Recently, a highly conserved family of vesicular glutamate transporters, consisting of VGLUT1, VGLUT2 and VGLUT3, has been cloned and functionally characterized (review Fremeau et al., 2004). These transporters are mainly localized on the membrane of synaptic vesicles in glutamatergic neurons, but they are also present in astrocytes (Montana et al., 2004). In neurons they mediate glutamate uptake from the presynaptic lumen into the vesicles. The uptake is driven by a proton-based electrochemical gradient generated by a vacuolar H⁺-ATPase. The three transporters share high sequence similarities (VGLUT1 and VGLUT2 have a 82% amino acid identity and 92% similarity). They are also highly similar with respect to substrate specificity, kinetics and pharmacology. They only recognize glutamate, but not aspartate and show a biphasic dependence on chloride concentration. In contrast to these similarities, *in situ* hybridization experiments reveal a complementary expression pattern in the adult brain. VGLUT1 is predominantly found in the cerebral cortex, hippocampus and cerebellum, whereas VGLUT2 is prominent in diencephalon, brainstem and spinal cord. Although the majority of neurons express only one isoform, some co-expression has been described e.g. in primary sensory neurons or cerebellar mossy fiber terminals (Fremeau et al., 2001). Surprisingly, VGLUT3 is found mainly in neurons not considered to be glutamatergic, but cholinergic, serotonergic or GABAergic. Also, its

subcellular localization differs from its two relatives. While VGLUT1 and VGLUT2 are mostly found in nerve terminals, VGLUT3 is additionally localized in cell somata and dendrites, suggesting further roles for glutamate, e.g. in retrograde synaptic signaling (Fremeau et al., 2002).

Interestingly, VGLUT1 and VGLUT2 undergo transcriptional regulation during development resulting in a switch from VGLUT2 to VGLUT1 expression in the hippocampus, cortex and cerebellum. In the cerebellum for example, VGLUT2 is predominantly found in parallel and climbing fibers at early postnatal stages and starts to be downregulated at postnatal day 7 while VGLUT1 starts to be upregulated at the same time. Around postnatal day 30, VGLUT1 is the most prominent vesicular glutamate transporter found in the cerebellum whereas VGLUT2 only remains present in climbing fibers (Miyazaki et al., 2003). The reason for the developmental switch in transporter subtypes and for their complementary expression pattern in the adult organism is not yet fully understood. One possible explanation could be the mode of glutamate release of the synapses the transporters are located to. VGLUT1 is mostly found at synapses showing a low probability of transmitter release, while VGLUT2 is localized to synapses with a higher release probability. Thus, both transporters may contribute to different aspects of synaptic transmission beyond their identified role of glutamate uptake (review Fremeau et al., 2004).

In the present work we found reduced levels of VGLUT in neurons lacking both *app* and *aplp2*. Due to possible antibody cross-reactivity across the different VGLUT isoforms, we were not able to unambiguously identify the affected VGLUT isoform at the protein level. However, the quantitative RT-PCR data strongly suggest that *vglut2* transcription is clearly and specifically downregulated in *app*^{-/-} *aplp2*^{-/-} neurons, while *vglut1* transcription was comparably low in both wild-type and double knock-out neurons. Therefore, we conclude that the observed reduction of vesicular glutamate transporter can largely be attributed to altered expression of the VGLUT2 isoform. The low detection of *vglut1* transcript in our neurons after 12 DIV is consistent with the reported developmental switch from VGLUT2 to VGLUT1 occurring in postnatal neurons *in vivo*, as the neurons probably did not yet reach the developmental stage *in vitro* where the subtype switch takes place. The changes in *vglut2* transcription were observed after the neurons had been in culture for at least 12 days. At this time point a clear decrease of transcription was detected in the double knock-out neurons. We did not investigate if this decrease represents a massive delay in development that would subsequently reach wild-type levels at later time points or if we observe a permanent downregulation. This question is of particular

importance in the context of future *in vivo* work. Indeed, in our cell culture system neuronal differentiation occurs largely in a synchronous manner which facilitates the kind of observations reported here. But *in vivo*, diverse neuronal populations differentiate at rates that regionally differ, a feature that could potentially complicate the analysis of transient versus permanent changes in gene expression. Initially, we also included the *app* single knock-out cells in our study and observed a decrease in VGLUT2 protein level that was less clear than the decrease observed in neurons lacking *app* and *apl2*. In addition, the protein levels of VGLUT2 in the *app*^{-/-} neurons showed substantial variations between experiments, perhaps as a consequence of the suspected partial redundancy between the three members of the family. In view of this, we only performed a limited number of experiments with the *app* single knock-out cells.

Of special relevance to the present work is the demonstration that the amount of glutamate transported in synaptic vesicles depends on the number of VGLUT1 molecules present per vesicle (Wilson et al., 2005). The amount of released glutamate can therefore be at least in part dictated by the number of VGLUT transporter molecules. The expression of the transporter itself is developmentally regulated, activity-dependent and furthermore increases during synapse maturation. This suggests the existence of a mechanism by which VGLUT could regulate the functional dynamic range of glutamatergic synapses. Recently, the role of VGLUT1 in excitatory transmission has been clearly demonstrated by deletion of the *vglut1* gene in mice (Fremeau et al., 2004; Wojcik et al., 2004). The absence of the transporter resulted in either silent synapses or synapses with reduced spontaneous or evoked responses. Comparable studies with mice lacking *vglut2* have not been published so far.

Our observation that decreased levels of vesicular glutamate transporter in neurons lacking *app* and *apl2* result in less glutamate release is in line with the results obtained by Wilson et al. (2005). The reduced levels of *vglut2* transcripts can be expected to result in less transporter present in the vesicles which is likely to influence the uptake and release of glutamate. In line with this, following loading of our cells with ³[H]-labeled glutamate, we found that less glutamate was released after application of depolarizing concentrations of KCl or glutamate. As could be expected, the release was not fully abolished since detectable levels of transporters were still found in double knock-out neurons. The reduced transmission did not change the survival of the neurons since we were able to keep them in culture for similar time periods as the wild-type cells without observing obvious signs of cell death. However, as glutamate is the most prominent neurotransmitter in the nervous system changes in its

availability at certain time points of development *in vivo* might result in severe synaptic dysfunctions that can conceivably compromise the survival of newborn animals in the first weeks after birth. The absence of the *vglut1* gene, for example, results in lethality of the animals between postnatal day 18 and 21 (Wojcik et al., 2004). While they display no abnormalities in the first two weeks after birth compared to their littermates, the animals start to differ with the beginning of the third week. They lag behind in growth, develop movement disorders and emaciate. Although the cause of death remains unclear it occurs around the time when the subtype switch from VGLUT2 to VGLUT1 takes place. The survival of the VGLUT1 deficient animals until the end of the third postnatal week and the normal development during the first two weeks, emphasizes the predominance of VGLUT2 driven glutamatergic transmission during early brain maturation. The progressive lack of glutamate transmission in areas of the brain such as the hippocampus and the cortex, as well as in peripheral systems could result in malfunction of organs, leading to the lethal phenotype of the animals.

Taken together, the vesicular glutamate transporters seem to play a crucial role during early brain development and reduced levels are likely to lead to severe synaptic dysfunction. Therefore, the observed decrease of VGLUT2 expression in the absence of *app* and *aplp2* could be one explanation for the early postnatal lethality of the *app*^{-/-} *aplp2*^{-/-} mice.

Indeed, the parallels between the *app*^{-/-} *aplp2*^{-/-} and the *vglut1*^{-/-} animals are intriguing, as both mouse models show a lethal phenotype without displaying gross histological abnormalities in the brain or other organs. Recent studies performed with *app*^{-/-} *aplp2*^{-/-} animals (Wang et al., 2005; Yang et al., 2005; Chapter 4.4 of the Discussion) revealed a presynaptic phenotype that results in changes of synaptic transmission and reduced synaptic vesicle numbers in synapses of neuromuscular junctions and submandibular ganglia. Changes in synaptic transmission and reduced numbers of synaptic vesicles have been shown for *vglut1*^{-/-} animals as well (Freneau et al., 2004; Wojcik et al., 2004).

Experiments to confirm the decrease of *vglut2* transcription in the *app*^{-/-} *aplp2*^{-/-} animals are currently in progress.

Glutamate transmission and vesicular glutamate transporters are also involved in mechanisms outside the central nervous system. For example, there is compelling evidence for the expression and function of glutamate as a signaling molecule in the digestive system (review Li et al., 2005). Recently, presence of VGLUT1 and VGLUT2 in the enteric nervous system and pancreatic tissue has been reported. Glutamate release seems to be involved in modulation of digestive mechanisms such as acid secretion

in the stomach or contractility in the gastrointestinal tract. In the pancreas, glutamate has been found to act as an intracellular messenger in glucose-induced insulin exocytosis and glucagon exocytosis. VGLUT1 and VGLUT2 were shown to be differentially regulated by glucose levels in pancreatic cells and seem to take part in the regulated secretion of insulin (review Li et al., 2005). The recent evidence for glutamate and VGLUTs being involved in non-neuronal pathways such as hormone release, might provide an additional explanation for the lethality of the *vglut1*^{-/-} animals. The absence of VGLUT1 in pancreatic tissue could lead to changes in hormone secretion resulting in the shutdown of organs. Thus, the lethal phenotype of *vglut1* knock-out animals could be the result of an accumulation of several disrupted glutamate release mechanisms, both neuronal and non-neuronal. The same could hold true for the *app*^{-/-} *aplp2*^{-/-} animals.

4.2 Changes of PSD-95 in neurons lacking *app* and *aplp2*

In addition to the reduced expression of the presynaptically localized VGLUT2, we observed decreased levels of the postsynaptic protein PSD-95 (postsynaptic density-95) in neurons lacking *app* and *aplp2*. PSD-95 is part of a highly organized structure found adjacent to the postsynaptic membrane of excitatory synapses. It is involved in the structural organization of postsynaptic signaling complexes by interaction with membrane proteins such as NMDA receptors and cytoplasmic signaling molecules. In particular, it is involved in processes of synapse assembly and maturation as well as synaptic transmission and plasticity (Kim et al., 2004). We did not further investigate the changes of PSD-95 in our system as we decided to focus on the more prominent decrease of the vesicular glutamate transporter. In particular, we do not know at this time point if the reduced expression of PSD-95 is a consequence of the presynaptic alterations or if it is a process occurring independently from the *vglut2* phenotype. However, in addition to the presynaptic alteration, based on the PSD-95 data we suspect that the function of excitatory synapses may be affected in the absence of *app* and *aplp2* as a result of both pre- and postsynaptic changes.

4.3 The APP intracellular domain and transcriptional modulation

The observed decrease in *vglut2* transcription raises the question of a possible mechanistic link between these changes and the presence or absence of *app* and *aplp2*. Recently, the existence of a small (6 kDa) C-terminal fragment, called APP intracellular domain (AICD), has been reported (Passer et al., 2000). The AICD is generated by proteolytic cleavage at the ϵ -cleavage site, located ~ 7 amino acids next to the amyloid β cleavage site, in the transmembrane region of the protein. Its generation is presenilin-dependent and most publications referred to it as γ -secretase mediated cleavage, although there is some evidence for γ - and ϵ - independent catalytic events (Chen et al., 2002; Kume et al., 2004). For simplicity, we will refer to γ -secretase mediated cleavage when referring to the generation of AICD.

In analogy with Notch, AICD is thought to mediate a similar signaling function for APP and its relatives. Notch is a type I transmembrane protein, acting as a membrane-bound transcription factor that regulates cell-fate determination during development (review Selkoe & Kopan, 2003). The heterodimeric-receptor Notch is targeted to the cell surface. After binding to its ligands from the Delta/Jagged family, two subsequent cleavages occur mediated by metalloproteases of the ADAM family and γ -secretase respectively, finally resulting in the release of the Notch intracellular domain (NICD) into the cytoplasm. The NICD translocates to the nucleus and associates with a DNA-binding protein called CSL (CBF1, Suppressor of Hairless and Lag-1). In the absence of the NICD, CSL acts as repressor of transcription and is bound to several proteins such as SMRT (Silencing Mediator of Retinoid and Thyroid hormone receptor) and HDAC (histone deacetylase). Upon binding of NICD to CSL, the latter converts from a transcriptional repressor to an activator. The SMRT/HDAC complex dissociates and histone acetylases can be recruited to assist chromatin remodeling and initiate transcription of target genes such as HES genes. The signaling function of the NICD is controlled by phosphorylation and ubiquitination that results in the degradation of the intracellular domain and resets the cell again to a basal state until the next signaling cascade is started.

The elucidation of the Notch signaling pathway provided the basis for further work related to the possible mechanism used in the context of APP signaling. The first evidence for a role of the AICD in transcriptional regulation was obtained by Cao et al. (2001) using a heterologous reporter system. Fusion of APP with DNA binding domains of either yeast (Gal4) or bacterial (LexA) transcription

factors resulted in transcriptional activation in cell lines, when co-transfected with the APP adaptor protein Fe65 and the histone acetyltransferase Tip60. Although the exact mechanism is not fully understood yet, the experiments of Cao et al. (2001 and 2004) suggest the following mechanism (Fig. 26):

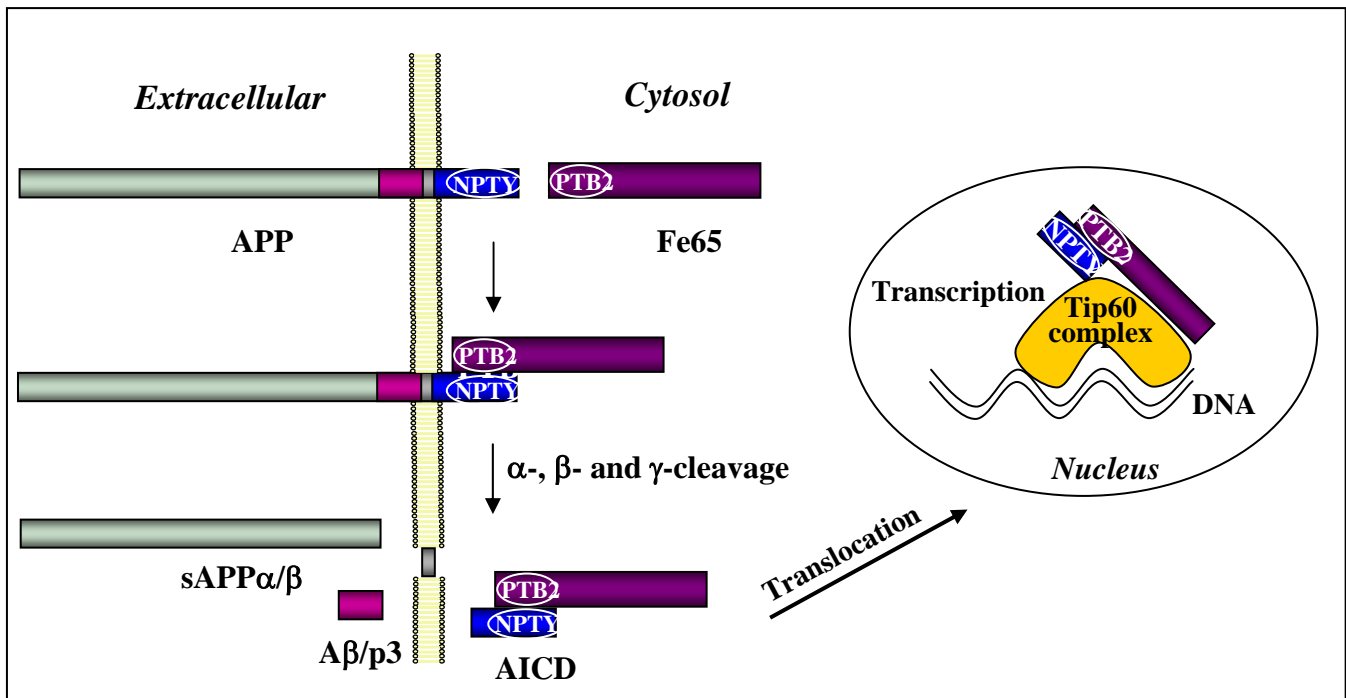


Figure 26: Working model for the function of AICD regulated transcription

When membrane-bound, APP binds to the phosphotyrosine-binding domain 2 (PTB2) of its adaptor protein Fe65 via its conserved NPTY domain at the C-terminus. Cleavage by α -, β - and γ -secretase takes place and the AICD/Fe65 complex is released into the cytoplasm. It translocates to the nucleus where Fe65 binds to the histone acetyltransferase Tip60 and transcription of genes is initiated.

The AICD acts outside the nucleus as a membrane-tethered recruiting device for Fe65, comparable with the Notch CSL. Fe65 binds via its PTB (phosphotyrosine-binding) domain to a conserved NPTY motif in the C-terminus of the AICD and stabilizes it. The AICD needs to be membrane-bound to be able to bind Fe65. Cleavage by γ -secretase releases the AICD-Fe65 complex, which then translocates to the nucleus where Fe65 binds to Tip60 and initiates transcription. According to their sequence similarities, it is not surprising that APLP1 and APLP2 also release an intracellular domain after γ -secretase cleavage. The APP-like intracellular domains 1 and 2 (ALICD1 and ALICD2) have also been shown to modulate gene transcription by forming a complex with Fe65 and Tip60 (Scheinfeld et al., 2002).

So far, several target genes of AICD transcriptional regulation have been identified. Most of them are linked to APP turnover itself, such as APP, β -secretase and Tip60 (von Rotz et al., 2004). However, KAI1, another target gene, has no link to APP or Alzheimer's disease (Baek et al., 2002). Recently, the amyloid β degrading enzyme neprilysin has been identified as a target gene (Pardossi-Piquard et al., 2005). Interestingly, its transcriptional regulation is not only controlled by the presence of the APP intracellular domain but also by the intracellular domains of APLP1 and APLP2. The authors could demonstrate that in the absence of *app* and *aplp2* the decrease of neprilysin transcription was much stronger than in the absence of either gene alone. This favours a synergistic effect of both intracellular domains and argues for a partly redundant function of both proteins.

While most of the studies on AICD have been performed with AICD overexpressing cell lines, very recently, Kimberly et al. (2005) were able to detect endogenous AICD in primary neuronal cultures. Neurons are known to express high amounts of APP which enabled the authors to detect the labile intracellular fragment and to demonstrate that it undergoes a temporally restricted upregulation. The highest levels of AICD in the neurons were found after they had been in culture for 5 to 7 days. During this peak of AICD generation a sub-fraction was detected in the nucleus, suggesting its contribution in specific transcriptional events. The levels of the fragment decreased rapidly thereafter because of phosphorylation of APP C-terminal fragments (CTFs) by C-Jun N-terminal kinase 3 (JNK3). The phosphorylation prevents binding of AICD and Fe65 and results in AICD degradation. The short time period in which the AICD levels are upregulated coincide with the onset of synapse formation, leading the authors to suggest a role for AICD in synaptogenesis. Clearly, our results are in agreement with this hypothesis and transcriptional activation by AICD may provide a mechanism by which *vglut2* transcription could be regulated. Additional support comes from the observation that treatment of wild-type neurons with a γ -secretase inhibitor resulted in the downregulation of *vglut2* transcription while another synaptic marker, synaptophysin, was not affected. The treatment of the neurons after 6 days in culture for a time period of 6 days revealed a consistent downregulation of *vglut2* transcription, while the treatment after 11 DIV showed more variations. This effect might be explained by the reported upregulation of AICD in primary neurons after 5-7 days in culture. In addition, the time period of inhibition could be crucial as well. A treatment with γ -secretase inhibitor for 6 days might result in a substantial decrease of AICD levels and AICD mediated transcription. However, treatment for 24 hours might not be long enough to sufficiently decrease AICD levels in order to detect a similar effect on transcription.

To further support a direct link between APP and VGLUT2 expression we are currently attempting to express AICD in ES cells lacking *app* and *aplp2*.

In addition to the effects obtained in the absence of APP and APLP2 we investigated whether *vglut2* transcription levels are increased in the presence of additional APP. As has been described (Bibel et al., 2004) APP is expressed already in neural progenitors in our system and its levels increase during the course of differentiation. By making use of neurons derived from ES cells expressing human APP driven by the endogenous *tau* promoter, we studied *vglut2* transcription after 5-6 days *in vitro*. This represents the time point when VGLUT2 protein starts to be clearly detectable and APP did not yet reach a stable expression level. These time points happen to coincide with those time points Kimberly et al. (2005) reported the highest amount of AICD present in neurons. Although we were able to observe an increase of *vglut2* transcription after 6 DIV we were not able to detect significantly increased amounts of total APP protein in the genetically modified neurons. Therefore we are not able to unambiguously link the observed effect on *vglut2* transcription to the additional presence of human APP. We can only speculate according to the findings of Kimberly et al. that a small additional amount of APP at the time point of highest AICD generation could result in a significant change of transcription.

4.4 Synaptic changes in mice lacking *app* and *aplp2*

The likelihood that both APP and APLP2 may be involved in synaptic function, possibly in a partly redundant fashion, was supported by two recent reports illustrating interesting structural changes in synapses of mice deficient in *app* and *aplp2* (Wang et al., 2005; Yang et al., 2005). Although the synaptic architecture in these animals had already been examined to some extent by Heber et al. (2000) and no apparent differences in synapse density or ultrastructure were reported, the recent studies did provide evidence for reduced numbers of synaptic vesicles and reduced size and number of active zones at synapses of neuromuscular junctions and submandibular ganglia. The structural abnormalities led to functional impairments in synaptic transmission. In addition, the development of neuromuscular junctions appears to be disrupted in the double knock-out animals. Reduced levels of presynaptic

markers such as synaptophysin and synapsin were observed, as well as increased sprouting of nerve terminals (Wang et al., 2005). The latter observations are consistently found in animals with retarded development of their neuromuscular junctions. In view of the possible role of APP as a kinesin-1 cargo receptor (see Introduction, Kamal et al., 2000, 2001), these findings suggest that the lack of APP may disturb proper axonal trafficking, resulting in fewer synaptic vesicles present at the neuromuscular endplate. However, Wang et al. (2005), directly addressed this question in the double knock-out animals but failed to obtain any evidence for alterations of axonal transport. The axonal structures looked normal and did not show signs of swellings (so called “axonal clogging”), caused by organelle accumulation, as has been demonstrated to occur in cells with disrupted transport mechanisms (Gunawardena et al., 2001).

Our observations that the absence of *app* and *aplp2* results in changes of synapse maturation and function of glutamatergic synapses is in general agreement with the findings of Wang et al. (2005) and Yang et al. (2005), even though their observations were largely based on a different methodology, involving for the most part immunocytochemical and electrophysiological methods.

Taken together, these two sets of observations suggest that in the combined absence of APP and APLP2, the development of both CNS glutamatergic and PNS cholinergic synapses may be retarded, perhaps as a result of delayed transcription of the corresponding target genes. In future experiments it will be interesting to examine the generality of this hypothesis linking genes of the APP family and synaptic function. This work may shed light not only on the physiological function of the APP-related genes, but also on the role of APP in pathological situations. It is now widely thought that besides A β plaques and neurofibrillary tangles, synaptic dysfunctions may be an early function-related event in AD, long before A β plaque formation can be detected (Selkoe et al., 2002). The findings of the present study might provide insight into the mechanisms that mediate synaptic changes in Alzheimer’s disease. At least for some cases of early familiar Alzheimer’s disease (FAD) a link between mutations in presenilin-1 and AICD generation has been demonstrated. Most of these mutations result in increased production of A β whereas the AICD generation is surprisingly decreased or even suppressed (Chen et al., 2002; Möhlmann et al., 2002). Thus, synaptic dysfunction in AD might be mediated by long-term alterations in AICD related transcription of the corresponding genes.

References

- Baek, S.H., Ohgi, K.A., Rose, D.W., Koo, E.H., Glass, C.K. and Rosenfeld, M.G. (2002). Exchange of N-CoR corepressor and Tip60 coactivator complexes links gene expression by NF- κ B and β -amyloid precursor protein. *Cell* 110, 55-67.
- Bibel, M., Richter, J., Schrenk, K., Staiger, V., Korte, M. and Barde, Y.-A. (2004). Differentiation of mouse embryonic stem cells into a defined neuronal lineage. *Nat. Neurosci.* 7, 1003-1008.
- Brewer, G.J. and Cotman, C.W. (1989). Survival and growth of hippocampal neurons in defined medium at low density: advantages of a sandwich culture technique or low oxygen. *Brain Res.* 494, 65-74.
- Caille, I., Allinquant, B., Dupont, E., Bouillot, C., Langer, A., Müller, U. and Prochiantz, A. (2004). Soluble form of amyloid precursor protein regulates proliferation of progenitors in the adult subventricular zone. *Development* 131, 2173-2181.
- Cao, X. and Südhof, T.C. (2001). A transcriptionally active complex of APP with Fe65 and histone acetyltransferase Tip60. *Science* 293, 115-120.
- Cao, X. and Südhof, T.C. (2004). Dissection of amyloid- β precursor protein-dependent transcriptional transactivation. *J. Biol. Chem.* 279, 24601-24611.
- Chen, F., Gu, Y.J., Hasegawa, H., Ruan, X., Arawaka, S., Fraser, P., Westaway, D., Mount, H. and St. George-Hyslop, P. (2002). Presenilin 1 mutations activate γ_{42} -secretase but reciprocally inhibit ϵ -secretase cleavage of amyloid precursor protein (APP) and S3-cleavage of Notch. *J. Biol. Chem.* 277, 36521-36526.
- Chomczynski, P. and Sacchi, N. (1987). Single-step method of RNA isolation by acid guanidinium thiocyanate-phenol-chloroform extraction. *Anal. Biochem.* 162, 156-159.
- Coulson, E.J., Paliga, K., Beyreuther, K. and Masters, C.L. (2000). What the evolution of the amyloid precursor supergene family tells us about its function. *Neurochem. Int.* 36, 175-184.
- de Strooper, B. and Annaert, W. (2000). Proteolytic processing and cell biological functions of the amyloid precursor protein. *J. Cell Sci.* 113, 1857-1870.
- de Strooper, B. (2003). Aph-1, Pen-2, and nicastrin with presenilin generate an active γ -secretase complex. *Neuron* 38, 9-12.

- Evans, M.J. and Kaufman, M.H. (1981). Establishment in culture of pluripotent cells from mouse embryos. *Nature* 292, 154-156.
- Freneau, R.T., Troyer, M.D., Pahner, I., Nygaard, G.O., Tran, C.H., Reimer, R.J., Bellocchio, E.E., Fortin, D., Storm-Mathisen, J. and Edwards, R.H. (2001). The expression of vesicular glutamate transporters defines two classes of excitatory synapse. *Neuron* 31, 247-260.
- Freneau, R.T., Burman, J., Qureshi, T., Tran, C.H., Proctor, J., Johnson, J., Zhang, H., Sulzer, D., Copenhagen, D.R., Storm-Mathisen, J., Reimer, R.J., Chaudhry, F.A. and Edwards, R.H. (2002). The identification of vesicular glutamate transporter 3 suggests novel modes of signaling by glutamate. *Proc. Natl. Acad. Sci. USA*. 99, 14488-14493.
- Freneau, R.T., Voglmaier, S., Seal, R.P. and Edwards, R.H. (2004). VGLUTs define subsets of excitatory neurons and suggest novel roles for glutamate. *Trends Neurosci.* 27, 98-103.
- Freneau, R.T., Kam, K., Qureshi, T., Johnson, J., Copenhagen, D.R., Storm-Mathisen, J., Chaudhry, F.A., Nicoll, R.A. and Edwards, R.H. (2004). Vesicular glutamate transporters 1 and 2 target to functionally distinct synaptic release sites. *Science* 304, 1815-1819.
- Griesbeck, O., Canossa, M., Campana, G., Gärtner, A., Hoehner, M., Nawa, H., Kolbeck, R. and Thoenen, H. (1999). Are there differences between the secretion characteristics of NGF and BDNF? Implications for the modulatory role of neurotrophins in activity-dependent neuronal plasticity. *Microsc. Res. Tech.* 45, 262-275.
- Gunawardena, S. and Goldstein, L.S. (2001). Disruption of axonal transport and neuronal viability by amyloid precursor protein mutations in *Drosophila*. *Neuron* 32, 389-401.
- Heber, S., Herms, J., Gajic, V., Hainfellner, J., Aguzzi, A., Rüllicke, T., Kretschmar, H., von Koch, C., Sisodia, S.S., Tremml, P., Lipp, H.-P., Wolfert, D. and Müller, U. (2000). Mice with combined gene knock-outs reveal essential and partially redundant functions of amyloid precursor protein family members. *J. Neurosci.* 20, 7951-7963.
- Kamal, A., Stokin, G.B., Yang, Z., Xia, C.H. and Goldstein, L.S. (2000). Axonal transport of amyloid precursor protein is mediated by direct binding to the kinesin light chain subunit of kinesin-I. *Neuron* 28, 449-459.
- Kamal, A., Almenar-Queralt, A., LeBlanc, J.F., Roberts, E.A. and Goldstein, L.S.B. (2001). Kinesin-mediated axonal transport of a membrane compartment containing β -secretase and presenilin-1 requires APP. *Nature* 414, 643-648.
- Kamenetz, F., Tomita, T., Hsieh, H., Seabrook, G., Borchelt, D., Iwatsubo, T., Sisodia, S.S. and Malinow, R. (2003). APP processing and synaptic function. *Neuron* 37, 925-937.
- Kim, E. and Sheng, M. (2004). PDZ domain proteins of synapses. *Nat. Rev. Neurosci.* 5, 771-781.

- Kim, T.W., Wu, K., Xu, J.L., McAuliffe, G., Tanzi, R.E., Wasco, W. and Black, I.B. (1995). Selective localization of amyloid precursor-like protein 1 in the cerebral cortex postsynaptic density. *Brain Res. Mol. Brain Res.* *32*, 36-44.
- Kimberly, W.T., Zheng, J.B., Town, T., Flavell, R.A. and Selkoe, D.J. (2005). Physiological regulation of the β -amyloid precursor protein signaling domain by c-Jun N-Terminal Kinase JNK3 during neuronal differentiation. *J. Neurosci.* *25*, 5533-5543.
- Kirazov, E., Kirazov, L., Bigl, V. and Schliebs, R. (2001). Ontogenetic changes in protein level of amyloid precursor protein (APP) in growth cones and synaptosomes from rat brain and prenatal expression pattern of APP mRNA isoforms in developing rat embryo. *Intern. J. Dev. Neurosci.* *19*, 287-296.
- Koo, E.H., Sisodia, S.S., Archer, D.R., Martin, L.J., Weidemann, A., Beyreuther, K., Fischer, P., Masters, C.L. and Price, D.L. (1990). Precursor of amyloid protein in Alzheimer disease undergoes fast anterograde axonal transport. *Proc. Natl. Acad. Sci. USA.* *87*, 1561-1565.
- Kume, H., Maruyama, K. and Kametani, F. (2004). Intracellular domain generation of amyloid precursor protein by epsilon-cleavage depends on C-terminal fragment by alpha-secretase cleavage. *Int. J. Mol. Med.* *13*, 121-125.
- Larbig, G., Zall, A. and Schmidt, B. (2004). Inhibitors designed for Presenilin1 by means of aspartic acid activation. *Helvetica Chimica Acta* *87*, 2334-2340.
- Li, T., Ghishan, F.K. and Bai, L. (2005). Molecular physiology of vesicular glutamate transporters in the digestive system. *World J. Gastroenterol.* *11*, 1731-1736.
- Li, Q. and Südhof, T.C. (2004). Cleavage of APP and APLP's by BACE 1. *J. Biol. Chem.* *279*, 10542-50.
- Li, Z.W., Stark, G., Götz, J., Rüllicke, T., Müller, U. and Weissmann, C. (1996). Generation of mice with a 200-kb amyloid precursor protein gene deletion by Cre recombinase-mediated site-specific recombination in embryonic stem cells. *Proc. Natl. Acad. Sci. USA.* *93*, 6158-6162.
- Lo, A.C., Thinakaran, G., Slunt, H.H. and Sisodia, S.S. (1995). Metabolism of the amyloid precursor-like protein 2 in MDCK cells. Polarized trafficking occurs independent of the chondroitin sulfate glycosaminoglycan chain. *J. Biol. Chem.* *270*, 12641-12645.
- Lorent, K., Overbergh, D., Moechars, B., de Strooper, F., van Leuven, F. and van den Berghe, H. (1995). Expression in mouse embryos and in adult mouse brain of three members of the alpha-2-macroglobulin receptor/low density lipoprotein receptor-related protein and of its ligands apolipoprotein E, lipoprotein lipase, alpha-2-macroglobulin and the 40000 molecular weight receptor associated protein. *Neuroscience* *65*, 1009-1025.
- Malatesta, P., Hack, M.A., Hartfuss, E., Kettenmann, H., Klinkert, W., Kirchhoff, F. and Götz, M. (2003). Neuronal or glial progeny: regional differences in radial glial fate. *Neuron* *37*, 751-764.

- Miyazaki, T., Fukaya, M., Shimizu, H. and Watanabe, M. (2003). Subtype switching of vesicular glutamate transporters at parallel fiber-Purkinje cell synapses in developing mouse cerebellum. *Eur. J. Neurosci.* *17*, 2563-2572.
- Moehlmann, T., Winkler, E., Xia, X., Edbauer, D., Murrell, J., Capell, A., Kaether, C., Zheng, H., Ghetti, B., Haass, C. and Steiner, H. (2002). Presenilin-1 mutations of leucine 166 equally affect the generation of the Notch and APP intracellular domains independent of their effect on A β ₄₂ production. *Proc. Natl. Acad. Sci. USA* *99*, 8025-8030.
- Montana, V., Ni, Y., Sunjara, V., Hua, X. and Parpura, V. (2004). Vesicular glutamate transporter-dependent glutamate release from astrocytes. *J. Neurosci.* *24*, 2633-2642.
- Morimoto, T., Ohsawa, I., Takamura, C., Ishiguro, M. and Kohsaka, S. (1998). Involvement of amyloid precursor protein in functional synapse formation in cultured hippocampal neurons. *J. Neurosci. Res.* *51*, 185-195.
- Moya, K.L., Benowitz, L.I., Schneider, G.E. and Allinquant, B. (1994). The amyloid precursor protein is developmentally regulated and correlated with synaptogenesis. *Dev. Biol.* *161*, 597-603.
- Müller, U., Cristina, N., Li, Z.-W., Wolfer, D.P., Lipp, H.-P., Rüllicke, T., Brandner, S., Aguzzi, A. and Weissmann, C. (1994). Behavioral and anatomical deficits in mice homozygous for a modified β -amyloid precursor protein gene. *Cell* *79*, 755-765.
- Ohsawa, I., Takamura, C., Morimoto, T., Ishiguro, M. and Kohsaka, S. (1999). Amino-terminal region of secreted form of amyloid precursor protein stimulates proliferation of neural stem cells. *Eur. J. Neurosci.* *11*, 1907-1913.
- Paliga, K., Peraus, G., Kreger, S., Durrwang, U., Hesse, L., Multhaupt, G., Masters, C.L., Beyreuther, K. and Weidemann, A. (1997). Human amyloid precursor-like protein1 – cDNA cloning, ectopic expression in COS-7 cells and identification of soluble forms in the cerebrospinal fluid. *Eur. J. Biochem.* *250*, 354-363.
- Pardossi-Piquard, R., Petit, A., Kawarai, T., Sunyach, C., Alves da Costa, C., Vincent, B., Ring, S., D'Adamio, L., Shen, J., Müller, U., St. George-Hyslop, P and Checler, F. (2005). Presenilin-dependent transcriptional control of the A β -degrading enzyme neprilysin by intracellular domains of β APP and APLP. *Neuron* *46*, 541-554.
- Passer, B., Pellegrini, L., Russo, C., Siegel, R.M., Lenardo, M.J., Schettini, G., Bachmann, M., Tabaton, M. and D'Adamio, L. (2000). Generation of an apoptotic intracellular peptide by γ -secretase cleavage of Alzheimer's amyloid β protein precursor. *J. Alzheimers Dis.* *2*, 289-301.
- Perez, R.G., Zheng, H., van der Ploeg, L.H.T. and Koo, E.H. (1997). The β -amyloid precursor protein of Alzheimer's disease enhances neuron viability and modulates neuronal polarity. *J. Neurosci.* *17*, 9497-9414.

- Robertson, E.J. (1987). Teratocarcinomas and embryonic stem cell a practical approach. IRL Press Limited, Oxford, England
- Sabo, S.L., Ikin, A.F., Buxbaum, J.D. and Greengard, P. (2003). The amyloid precursor protein and its regulatory protein, FE65, in growth cones and synapses *in vitro* and *in vivo*. *J. Neurosci.* 23, 5407-5415.
- Scheinfeld, M.H., Ghersi, E., Laky, K., Fowlkes, B.J. and D'Adamio, L. (2002). Processing of β -amyloid precursor-like protein-1 and -2 by γ -secretase regulates transcription. *J. Biol. Chem.* 277, 44195-44201.
- Schmidt, B. (2003). Aspartic proteases involved in Alzheimer's disease. *Chem. Bio. Chem.* 4, 366-378.
- Schubert, W., Prior, R., Weidemann, A., Dirksen, H., Mulhaupt, G., Masters, C.L. and Beyreuther, K. (1991). Localization of Alzheimer beta A4 amyloid precursor protein at central and peripheral synaptic sites. *Brain Res.* 563, 184-194.
- Selkoe, D.L. (2002). Alzheimer's disease is a synaptic failure. *Science* 298, 789-791.
- Selkoe, D.J. and Podlisny, M.B. (2002). Deciphering the genetic basis of Alzheimer's disease. *Annu. Rev. Genomics Hum. Genet.* 3, 67-99
- Selkoe, D. and Kopan, R. (2003). Notch and presenilin: regulated intramembrane proteolysis links development and degeneration. *Annu. Rev. Neurosci.* 26, 565-597.
- Slunt, H.H., Thinakaran, G., von Koch, C., Lo, A.C.Y., Tanzi, R.E. and Sisodia, S.S. (1994). Expression of a ubiquitous, cross-reactive homologue of the mouse β -amyloid precursor protein (APP). *J. Biol. Chem.* 269, 2637-2644.
- Tanzi, R.E. and Bertram, L. (2005). Twenty years of Alzheimer's disease amyloid hypothesis: a genetic perspective. *Cell* 120, 545-555.
- Thinakaran, G., Kitt, C., Roskams, A.J., Slunt, H.H., Masliah, E., von Koch, C., Ginsberg, S.D., Ronnett, G.V., Reed, R.R., Price, D.L. and Sisodia, S.S. (1995). Distribution of an APP homolog, APLP2, in the mouse olfactory system: a potential role for APLP2 in axogenesis. *J. Neurosci.* 15, 6314-6326.
- Trapp, B.D. and Hauer, P.E. (1994). Amyloid precursor protein is enriched in radial glia: implications for neuronal development. *J. Neurosci. Res.* 37, 538-550.
- von Koch, C.S., Zheng, H., Chen, H., Trumbauer, M., Thinakaran, G., van der Ploeg, L.H.T., Price, D.L. and Sisodia S.S. (1997). Generation of APLP2 ko mice and early postnatal lethality in APLP2/APP double ko mice. *Neurobiol. Aging* 18, 661-669.

- von Rotz, R.C., Kohli, B.M., Bosset, J., Meier, M., Suzuki, T., Nitsch, R.M. and Konietzko, U. (2004). The APP intracellular domain forms nuclear multiprotein complexes and regulates the transcription of its own precursor. *J. Cell Sci.* *117*, 4435-4448.
- Wilson, N.R., Kang, J., Hueske, E.V., Leung, T., Varoqui, H., Murnick, J.G., Erickson, J.D. and Liu, G. (2005). Presynaptic regulation of quantal size by vesicular glutamate transporter VGLUT1. *J. Neurosci.* *25*, 6221-6234.
- Wang, P., Yang, G., Mosier, D.R., Chang, P., Zaidi, T., Gong, Y.D., Zhao, N.M., Dominguez, B., Lee, K.F., Gan, W.B. and Zheng, H. (2005). Defective neuromuscular synapses in mice lacking amyloid precursor protein (APP) and APP-like protein 2. *J. Neurosci.* *25*, 1219-1225.
- Wasco, W., Bupp, K., Magendantz, M., Gusella, J.F., Tanzi, R.E. and Solomon, F. (1992). Identification of a mouse brain cDNA that encodes a protein related to the Alzheimer disease-associated amyloid β protein precursor. *Proc. Natl. Acad. Sci. USA* *89*, 10758-10762.
- Wasco, W., Gurubhagavatula, S., Paradis, M., Romano, D.M., Sisodia, S.S., Hyman, B.T., Leve, R.L. and Tanzi, R.E. (1993). Isolation and characterization of APLP2 encoding a homologue of the Alzheimer's associated amyloid β protein precursor. *Nat. Genet.* *5*, 95-100.
- Wojcik, S.M., Rhee, J.S., Herzog, E., Sigler, A., Jahn, R., Takamori, S., Brose, N. and Rosenmund, C. (2004). An essential role for vesicular glutamate transporter 1 (VGLUT1) in postnatal development and control of quantal size. *Proc. Natl. Acad. Sci. USA.* *101*, 7158-7163.
- Yamazaki, T., Koo, E.H. and Selkoe, D.J. (1997). Cell surface amyloid β -protein precursor colocalizes with β 1 integrins at substrate contact sites in neural cells. *J. Neurosci.* *17*, 1004-1010.
- Yang, G., Gong, Y.-D., Gong, K., Jiang, W.-L., Kwon, E., Wang, P., Zheng, H., Zhang, X.-F., Gan, W.-B. and Zhao, N.-M. (2005). Reduced synaptic vesicle density and active zone size in mice lacking amyloid precursor protein (APP) and APP-like protein 2. *Neurosci. Lett.* *384*, 66-71.
- Zheng, H., Jiang, M., Trumbauer, M., Sirinathsinghji, D.J.S., Hopkins, R., Smith, D.W., Heavens, R.P., Dawson, G.R., Boyce, S., Conner, M.W., Stevens, K.A., Slunt, H.H., Sisodia, S.S., Chen, H.Y. and van der Ploeg, L.H.T. (1995). β -amyloid precursor protein-deficient mice show reactive gliosis and decreased locomotor activity. *Cell* *81*, 525-531.

Acknowledgements

I would like to thank my two supervisors, Dr. Miriam Bibel and Prof. Yves-Alain Barde for giving me the opportunity to work on this challenging and exciting project in the field of stem cell research. Thank you very much for your advice, support and patience. I enjoyed being involved in the establishment of this great differentiation method!

I would like to thank Prof. Markus Rüegg for his evaluation of my thesis.

I would like to thank Jens Richter for his excellent technical support (e.g. isolation of ES cells), for endless discussions regarding work and life, for mental support in times of desperation and for funny times in the lab.

I would like to thank Emmanuel Lacroix for his technical support regarding molecularbiological methods.

I would like to thank the members of our lab at Novartis and the members of the lab of Yves-Alain Barde at the biocenter for helpful comments and a friendly atmosphere.

I would like to thank Amanda Littlewood-Evans, Stefan (Meister) Wacha and Melanie Rittirsch – I would have been lost without having friends like you!

I would like to thank my parents, my brother and my sister for their support and understanding in all these years.

Finally, I would like to thank Jan-Erik Siemens for believing in me, for support and love with or without 10000 miles between us.

Curriculum Vitae

Name: Katrin Schrenk
Date of birth: 20.09.1973
Place of birth: Waldshut, germany
Nationality: german

Education

2001-2003 Begin of the PhD thesis at the Friedrich Miescher Institute in Basel, Neurobiology department, in the group of Prof. Yves-Alain Barde.

2003-present Continuation of the PhD thesis at the Novartis Pharma AG in Basel, Nervous System department, in the group of Dr. Miriam Bibel.

2000-2001 Industrial placement at Hoffman La-Roche in Basel, Neuroscience Department, in the group of Dr. Manfred Brockhaus.

1999-2000 Diploma thesis: *Influence of the protein kinase C on dendritic development of Purkinje Cells in organotypic slice cultures of mice.* Anatomical Institute Freiburg, AG “neuronal plasticity”, in the group of Prof. Josef Kapfhammer.

1994-2000 Study of Biology at the University Freiburg, Germany

1990-1993 Gymnasium, Germersheim, Germany

Scholarship

1994-2000 Studienstiftung des Deutschen Volkes